THESIS FOR THE DEGREE OF DOCTOR OF PHILOSOPHY IN ARCHITECTURE

Prestress and its application to shell, fabric, and cable net structures

ALEXANDER SEHLSTRÖM

Department of Architecture and Civil Engineering
Division of Architectural Theory and Methods
Architecture and Engineering Research Group
CHALMERS UNIVERSITY OF TECHNOLOGY

Göteborg, Sweden 2021

Cover:
Part of a minimal surface at some intermediate state between a catenoid and a helicoid given by the imaginary part of eq. (58) in Paper C with $\alpha \to \infty$ and $\beta = 0.2 + 0.8(1+i)/\sqrt{2}$.

Prestress and its application to shell, fabric, and cable net structures
Thesis for the degree of Doctor of Philosophy in Architecture
ALEXANDER SEHLSTRÖM
Department of Architecture and Civil Engineering
Division of Architectural Theory and Methods
Architecture and Engineering Research Group
Chalmers University of Technology

ABSTRACT

Prestressing and shells provide means to create material-efficient and well-functioning structures, as do their combination, offering opportunities for increased material efficiency within the built environment. Prestressing introduces stresses in an object to enhance its performance, and shells include concrete shells, masonry vaults, fabric structures, cable nets, and timber or steel gridshells. Both prestressing and shell structures come with technical and practical considerations that need attention during the design, or there is a risk of wasted opportunity. However, successful attention to and combination of these aspects, resulting in a material-efficient prestressed shell, is not enough to make a high-quality architecture. There is a need for additional project-specific considerations, requiring ways to study design choices' impact on structural and architectural aspects.

This thesis aims for an increased understanding of prestressing and its application to shell, fabric, and cable net structures and improved means for their design. It provides a broad overview of prestressing, expanding beyond the common perception of prestress being limited to concrete structures, and shell structures, focusing on applications within architecture. The scope is the combination of prestressing and shells, and it addresses three main research questions: (1) Can any shell be prestressed? For those that can, what is the meaning and influence of prestressing?; (2) How can prestressed shells be form-found using analytical and numerical approaches?; and (3) How can prestress in shells be represented and chosen, aspiring for efficient structural performance?

Appended papers A–F help answer these questions, and the thesis contributes to architectural and structural design and structural optimisation and applies differential geometry. It provides approaches for the form-finding of gridshells containing both tension and compression elements (Paper A) and of minimal surfaces (Paper C and D). Paper B concludes that a sphere cannot be actively prestressed, but a torus can. Paper E extends the Williams and McRobie (2016) discontinuous Airy stress function from flat structures to curved shells, allowing moments and shear forces in edge beams of shell structures to be quantified and appropriate prestressing chosen. Paper D uses a discrete Airy stress function and discusses the structural behaviour of shells with negative Gaussian curvature loaded with patch loads. Paper F studies Eduardo Torroja's prestressed concrete Alloz aqueduct, concluding that it acts as a beam rather than a shell, but also that longitudinal prestressing may reduce the wall bending moments and that, at some limit, the channel act as a cylindrical membrane-action shell rather than of an Euler-Bernoulli beam, enabling thinner cross-sections.

Keywords: Prestress, Geometric stiffness, Stress pattern, Conceptual design, Structural design, Form finding, Architecture, Engineering

Sammanfattning

Naturen visar att förspänning och skalstrukturer möjliggör materialeffektiva och välfungerande konstruktioner, så också deras kombination, och erbjuder möjligheter till ökad materialeffektivitet i den byggda miljön. Förspänning introducerar spänningar i ett objekt för att förbättra dess prestanda, och skal inkluderar betongskal, murade valv, textila konstruktioner, kabelnät och gitterskal av stål eller trä. Båda är förknippade med en uppsättning tekniska och praktiska utmaningar som kräver uppmärksamhet under utformningen, annars riskerar effektiviseringsmöjligheterna gå förlorade. Men även om ansträngningarna framgångsrikt resulterar i ett materialeffektivt förspänt skal är det inte tillräckligt för att skapa högkvalitativ arkitektur. För det krävs ytterligare projektspecifika överväganden under projekteringen, vilka är beroende av metoder för att studera designvals påverkan på konstruktion och arkitektur.

Denna avhandling syftar till en ökad förståelse för förspänning och dess tillämpning på skal-, textil- och kabelnätstrukturer och förbättrade tillvägagångssätt för deras utformning. Den ger en bred överblick över, å ena sidan, användning av förspänning, bortom den vanliga uppfattningen att förspänning endast är tillämplig på betongkonstruktioner, och, å andra sidan, skalkonstruktioner med fokus på tillämpning inom arkitektur. Fokus är kombinationen av förspänning och skal, och målet är att besvara följande huvudforskningsfrågor: (1) Kan alla skal förspännas? Vad är innebörden och inflytandet av förspänning för de som kan?; (2) Hur kan geometrin för förspända skal formsökas med hjälp av analytiska och numeriska metoder?; och (3) Hur kan förspänning i skal representeras och väljas, i strävan mot ett effektiv konstruktivt verkningssätt?

Sex bifogade artiklar bidrar till att svara på forskningsfrågorna. Avhandlingen bidrar till arkitektonisk och konstruktiv utformning samt strukturoptimering, och tillämpar differentialgeometri. Mer specifikt drar den slutsatsen att en sfär inte aktivt kan förspännas, men en torus kan (Artikel B). Den tillhandahåller metoder för att formsöka gitterskal med både tryckta och dragna element (Artikel A) och minimala ytor (Artikel C och D). Williams och McRobie (2016) diskontinuerliga version av Airys spänningsfunktion utvecklas från plana strukturer till krökta skal, så att moment och skjuvkrafter i skals kantbalkar kan kvantifieras och en lämplig förspänning väljas (Artikel E). Med hjälp av en diskontinuerliga Airys spänningsfunktion diskuteras verkningssättet hos skal med negativ Gausskrökning belastade med små ytlaster (Artikel D). Artikel F är en fallstudie om Eduardo Torrojas förspända betongakvedukt i Alloz, vilken konstaterar att akvedukten bättre beskrivs som en balk än ett skal, men också att en koncentrerad förspänningskraft i de längsgående kanterna är en förutsättning för jämvikt i böjspänningsfria cylindriska skal. Vidare minimerar denna förspänning böjmomentet i tvärsnittsväggen hos balkar med cylindriska tvärsnitt och, vid gränsen, är verkningssättet likt cylindriskt membranverkande skal snarare än en Euler-Bernoullibalk, vilket möjliggör tunnare tvärsnitt.

To Andreas

Devoting time and interest to deepened studies in a subject is a highly-rewarding intellectual endeavour that defines us as humans and has a value not despite but because of its practical uselessness.

— Hitz 2020

ACKNOWLEDGEMENTS

THESIS

This thesis consists of an extended summary and the following appended papers:

Paper A M. Ander et al. (2017). "Prestressed gridshell structures". *Proceedings of the International Association for Shell and Spatial Structures (IASS) Symposium 2017*

Paper B A. Sehlström and C. J. K. Williams (2019). "Unloaded prestressed shell formed from a closed surface unattached to any supports". *Proceedings of the International Association for Shell and Spatial Structures (IASS) Symposium 2019*

Paper C A. Sehlström and C. J. K. Williams (2021a). "Tensioned principal curvature cable nets on minimal surfaces". *Proceedings of the Advances in Architectural Geometry conference 2020*. Ed. by O. Baverel et al. Presses des Ponts, pp. 86–109

Paper D A. Sehlström and C. J. K. Williams (2021b). "The analytic and numerical form-finding of minimal surfaces and their application as shell structures". *Proceedings of the International Association for Shell and Spatial Structures (IASS) Symposium 2020/2021*

Paper E A. Sehlström, K.-G. Olsson, and C. J. K. Williams (2021a). Design of tension structures and shells using the Airy stress function. Accepted for publication

Paper F A. Sehlström, K.-G. Olsson, and C. J. K. Williams (2021b). Does Torroja's prestressed concrete Alloz aqueduct act as a beam or a shell? Under review (Third submission, 22 Nov 2021)

Author's contribution to jointly published papers

According to CRediT (Contributor Roles Taxonomy):

Paper A: Investigation, Software, Visualisation, Writing (original draft)

Paper B: Investigation, Software, Writing (original draft)

Paper C: Investigation, Visualisation, Writing (original draft, review & editing)

Paper D: Conceptualisation, Investigation, Software, Visualisation, Writing (original draft)

Paper E: Conceptualisation, Investigation, Methodology, Software, Validation, Visualisation, Writing (original draft, review & editing)

Paper F: Conceptualisation, Investigation, Methodology, Software, Validation, Visualisation, Writing (original draft, review & editing)

CONTENTS

Part I
Extended summary

1   Introduction

As evident in nature, for example, in spiderwebs and seashells, prestressing and shells provide means to create material-efficient and well-functioning structures, as do their combination. Prestressing introduces stresses in an object to enhance its performance, and shells include concrete shells, masonry vaults, fabric structures, cable nets, and timber or steel gridshells. Both prestressing and shells come with technical and practical considerations that need attention during the design, or there is a risk of wasted opportunity. This thesis combines the two, presenting research on prestressing and its application to shell, fabric, and cable net structures.

This chapter discusses the potential usage of prestressing and shell structures to meet global sustainability goals, accompanied by a discussion on the need for inter-disciplinary collaboration during design and to balance technical and non-technical aspects to create a piece of high-quality architecture. It defines the words *prestress*, *shell*, and *prestressed shell* and presents the aim of the research and general questions before introducing the scope, focusing the research on the application of prestressing on shell structures. The chapter concludes with the research objectives and a brief outline of the thesis organisation.

1.1   Build more with less

The UN predicts a global need to double the already built floor area until the year 2050–2060 to meet needs related to, for example, increased population, wealth, health, and urbanisation, meaning 'adding the equivalent of Paris to the planet *every single week* ... over the next 40 years' (UN 2017, p. 2). Constructing that many buildings and infrastructure requires a vast amount of construction materials, and if we are to accomplish this sustainably, we need to rethink the current way we design and construct our built environment. The rethinking has to occur on all levels, ranging from questioning, in broad terms, requirements for a prosperous and healthy life to, at the fine-grained level, developing and improving construction materials, and everything in between. For this, research and development are core activities, including studying our predecessors' approaches in a search for lost knowledge, leading to high-quality architecture and sound engineering solutions.

One of many ways forward is to increase the material efficiency of our structures—to build lightweight—so that the used materials work at a maximum at all points, allowing to build more with less.

The idea of building lightweight guided Frei Otto (1925–2015), resulting in an impressive range of work (Glaeser 1972) and research (Burkhardt 2016) that has inspired many architects, engineers, and researchers (Dixon 2015a; Dixon 2015b) and continuous to do so (Aldinger 2016). During the design of the 1972 Olympiastadion in Munich, consisting of a collection of post-tensioned cable net roofs, Otto worked together with a large team of experts (Tomlow 2016). One of them was Jörg Schlaich (1934–2021), whose own work since then has been in line with the idea of building more with less, proposing the application of five principles for the construction of material-efficient lightweight structures (J. Schlaich and M. Schlaich 2008):

1. Keep spans as short as possible

2. Use axial compression and tension—avoid bending

3. Use materials with a high ratio between tensile strength and density

4. Apply prestressing

5. Use curved geometry

The first three principles are straightforward to apply, although considering the environmental impact of the materials, for example, comparing embodied carbon equivalents, complicates the choice of material.

The fourth principle is about introducing stresses in an object to improve its performance during service. It is a simple and effective concept ubiquitous in nature and extensively used in everyday objects and load-bearing structures. However, its application results in several technical issues that often require special knowledge to address appropriately. Within the built environment, prestressing is primarily applied to concrete structures to, for example, reduce the need for reinforcement steel and to control creep (Menn 1990; Sanabra-Loewe and Capellà-Llovera 2014). Consequently, a common perception is that prestressing is only applicable to concrete, limiting the understanding of prestressing and the versatile possibilities that come with its application.

The fifth principle is to some extent an extension of the second; if the second principle means a beam dissolves into a truss and a plate into a space frame, the fifth principle transforms the truss into an arch or a cable, and the space frame into a shell, gridshell, membrane, or cable net structure. Requiring the curved structures to work without bending imposes additional geometrical constraints. Then Pucher's equation (Pucher 1938; Timoshenko and Woinowsky-Krieger 1959, p. 461), discussed in sections 3.3 and 3.4, describes the interplay between form and forces in loaded membrane-action curved structures, or membrane shells, for short. It involves three quantities defined on a plane: the form, or geometry, specified as the height z and the forces described by the internal membrane stress state ϕ and the loading q. Though Pucher's equation is valid only under certain circumstances, it helps us categorise the main structural challenges with the design of shells as *form-finding*, *stress-finding*, or even *load-finding*, although the latter is uncommon. Form-finding determines the geometry z given the desired stress state ϕ and a known loading q, whereas stress-finding solves ϕ given z and q. In any case, ϕ may represent a state of prestress. Pucher's equation is elegant and may appear simple, but the number of analytical solutions is limited and, in general, requires non-analytical, purpose-specific approaches to solve.

1.2 Design of efficient structures and high-quality architecture

Vitruvius proposed two thousand years ago that architecture should exhibit the three qualities of *utilitas*, *firmitas*, *venustas*—that is, utility/functionality, stability/sustainability, beauty (Vitruvius, Morgan, and Warren 1914). Characteristic for architecture that

possesses these qualities is holistic solutions of which the structure is just one of many contributing parts. While Schlaich's five principles for efficient structures may result in sound engineering solutions, it is necessary to balance these with other criteria to design a piece of architecture.

During Vitruvius's time, the design of buildings was a one-person-job done by a master builder or architect (from Greek *arkhi-*, chief, and *tekton*, builder). Today several professions share the design responsibility, with architects and engineers in the lead. The separation has enabled needed specialisation but also led to a fragmented design process (Sehlström, Ander, and Olsson 2021). Eugene-Emmanuel Viollet-le-Duc dwelled on the matter already in the late 19th century, concluding that 'the interest of the two professions will be best saved by their union' (Viollet-le-Duc 1881, p. 72). Improved collaboration may lead to such a union, and conceptual design is often put forward as a key to developing integrated qualitative architecture and sound engineering solutions (Gans 1991; Rice 1996; Larsen and Tyas 2003; Corres-Peiretti 2013). But architects and engineers 'tend to have different perceptions of the same reality' (Charleson and Pirie 2009), making successful collaboration challenging.

This dissertation departs from the firm belief that tools for exploring possibilities and representing phenomena enrich the design process and help improve collaboration. Then form-finding becomes more than precisely determining z of a shell; it serves as a tool to understand the implications of design choices and guide and inform new, leading to a well-argued proposal balancing and prioritising, often, contradicting criteria. Similarly, stress-finding extends beyond determining the forces the structure needs to resist and is instrumental for improving structural efficiency; it makes the interplay between form and forces tangible and allowing the understanding of the role of prestressing for the structural behaviour of shell structures.

1.3   Definitions

The word *prestress* compounds the prefix *pre-* and the stem *stress*, literary meaning 'before stress,' and is both a verb and a noun, therefore also an adjective. Some definitions of prestressing imply it is exclusive to concrete structures, while others limit the purpose of applying prestressing to counteract loads applied during service. However, such definitions are too limiting; prestressing may be applied independently on material and for many different reasons. This thesis uses the word *prestress* as follows.

> *prestress* (verb): to introduce internal stress into an object (during manufacture or before some other treatment or action) to improve its performance; in this sense, prestress is synonymous with prestressing.

> *prestress* (noun)   1: the stresses introduced in prestressing
>
> 2: the process of prestressing
>
> 3: the condition of being prestressed

Adriaenssens et al. (2014, p. 20) exclude tension-only structures from the definition of shells and require the structure to be 'relatively rigid,' leaving out structures such as sails,

balloons, and car tyres. But in this thesis, no such exclusion is made, and shells include less rigid tension structures such as fabric and cable net structures. The thesis uses the word *shell* and its synonym *shell structure* as follows.

> <u>*shell*</u> (<u>noun</u>): any curved thin structure that primarily resist loading through membrane action, the combination of compressive, tensile and shear stresses acting in the tangential plane of the surface.

Combining the above two definitions then give a definition for a *prestressed shell*.

> <u>*prestressed shell*</u> (<u>noun</u>): a shell with stresses introduced (during manufacture or before some other treatment or action) to improve its performance.

1.4   Aim and general questions

The application of prestressing and use of shell structures within the built environment provides opportunities for increased material efficiency, and so do their combination. Both come with a set of technical and practical considerations that need attention during design, or there is a risk of wasted opportunity. However, successful attention to and combination of these aspects, resulting in a material-efficient prestressed shell, fabric, or cable net, is not enough to make a qualitative piece of architecture. There is a need for additional project-specific considerations during design which requires ways to study the implication on structural and architectural aspects of design choices.

This thesis aims to provide an increased understanding of prestressing and its application to shell, fabric, and cable net structures and improved means for their design. With this backdrop, several general questions arise. When and how to apply to prestress? What possibilities to make structures more efficient does it offer? What approaches for the form-finding and stress-finding of shells are there? How to develop new ones? How shall tools work and representations look like to support increased understanding for the individual designer and improved collaboration between architects and engineers?

1.5   Scope

The scope of the presented studies focuses on the intersection of the fields of prestressing and shell structures. The scope effectively excludes studies, on the one hand, on some objectives with and applications of prestressing and, on the other, on shell structures that are not prestressed, as fig. 1.1 illustrates.

1.6   Research objectives

The understanding and application of prestressing are challenging endeavours on their own, and so is the design of shell structures. With the fields combined, further questions arise, and the objective of this research is to answer the following:
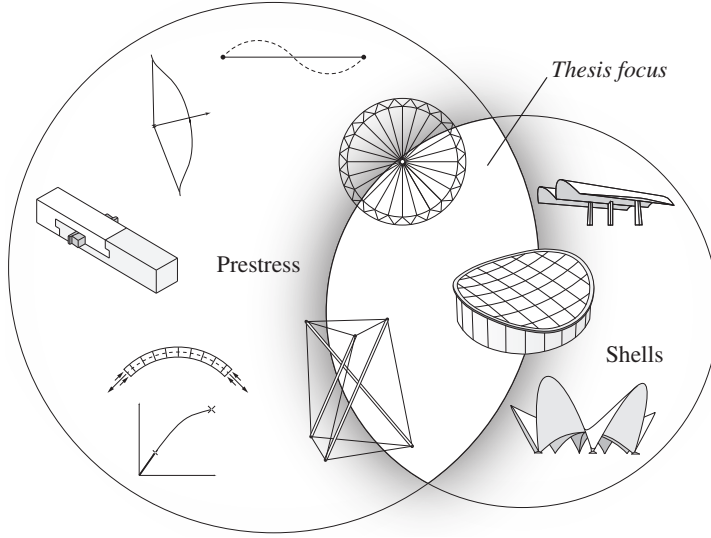
Figure 1.1: *Thesis focus: prestress as applied to shell structures, including concrete shells, masonry vaults, fabric structures, cable nets, and timber or steel gridshells*

1. Can any shell be prestressed? For those that can, what is the meaning and influence of prestressing?

2. How can prestressed shells be form-found using analytical and numerical approaches?

3. How can prestress in shells be represented and chosen, aspiring for efficient structural performance?

1.7   Thesis organisation

Part I begins with chapter 1 introducing the topic, aim, scope, and objectives. Chapters 2 and 3 contextualises prestressing and shell structures, respectively, before chapter 4 presents the chosen research methodology. Chapter 5 summarises the appended papers and chapter 6 conclude and present ideas for future works. Part II contain the six appended papers.

2 Prestress

Prestressing introduces internal stress into an object with the intention to improve its performance. Some immediate questions follow, such as when can prestressing be applied, how to prestress, and what performance improvements can it give? This chapter provides an overview of prestress as a concept, hopefully bringing some clarity to these questions.

2.1 Preliminaries

This section briefly discusses some fundamental physical concepts which are keys to understanding prestress and builds a framework of concepts enabling further discussions. Prestressing influences the geometric stiffness of a material object and, under certain conditions, the complete structure, affecting the response to loading. A statically determinate model of a structure cannot be prestressed, whereas a statically indeterminate can, and, under certain conditions, prestressing may render a mechanism rigid.

2.1.1 Stress

Stress is a physical quantity that arises within materials due to externally applied forces, uneven temperature, or permanent deformation. The measure for stress is force per unit area, although, when discussing thin shells, it is often more convenient to use stress resultants defined as the integrals of stress over the shell thickness, measured as force per unit width.

Six independent parameters arranged in a 3×3 matrix can, for any chosen Cartesian coordinate system, describe the state of stress at a material point. In case of a regular coordinate system where the coordinates are named x, y, z, the matrix may be written as

$$\begin{bmatrix} \sigma_x & \tau_{xy} & \tau_{xz} \\ \tau_{xy} & \sigma_y & \tau_{yz} \\ \tau_{xz} & \tau_{yz} & \sigma_z \end{bmatrix}, \tag{2.1}$$

where the components σ_x, σ_y, σ_z are the orthogonal normal stresses (for the considered coordinate system), and τ_{xy}, τ_{xz}, τ_{yz} the orthogonal shear stresses. Through a transformation of coordinates, it is always possible to find a Cartesian coordinate system such that all of the shear stress components are zero. Then the normal stresses are called principal stresses and the base vectors of the coordinate system point in principal stress directions. Normal and principal stresses are either tensile (positive) or compressive (negative).

For convenience, the description of the stress state is often simplified, ignoring the components that have an insignificant influence on the structural behaviour. For example, for a cable under tension, the stress state is usually sufficiently described by the normal stress acting along with the length direction.

All materials respond differently to stress. Except in the rare cases when Poisson's ratio is negative, tensile stress is related to a material extension in the associated direction,

whereas compressive stress is related to a shortening. Hence, tensile prestress, or pre-tension, is introduced by extending the material, whereas compressive prestress, or pre-compression, by compressing the material.

Stress cannot be measured directly and is, instead, determined by recalculating deformation measures into strains, after which, for example, Hook's law via experimentally determined material properties provide the stress.

2.1.2 Strength

The strength of a material is the limit under which the level of stress is safe, not causing (local) failure or plastic deformation. Brittle materials fail without plastic deformation, whereas ductile materials do (fig. 2.1); the latter failure is considered safer than the former in buildings since it gives some warnings in terms of large deformations before the collapse.

(a) *Brittle tension*   (b) *Brittle compression*   (c) *Ductile tension*   (d) *Ductile compression*
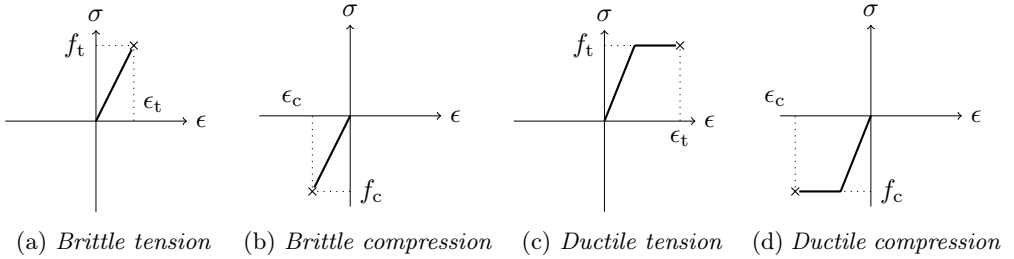
Figure 2.1: *Idealised characteristic constitutive material models relating strain ϵ to stress σ where f_t and f_c are the tensile and compressive strength, respectively, with corresponding strains ϵ_t and ϵ_c at failure*

2.1.3 Stiffness

Stiffness is the extent to which a material or structural object resists deformation in response to an applied force. Stiffness quantifies how much force has to be applied to cause a deformation.

For structural objects, stiffness may be understand as the sum of elastic and geometric stiffness. Elastic stiffness depends on material properties, geometry (shape, topology, cross-section), and boundary conditions, whereas geometric stiffness depends on the internal stress state. Compressive stresses result in a negative geometric stiffness contribution (weakening), while tensile stresses result in a positive geometric stiffness contribution (stiffening) (Olsson and Dahlblom 2016). If the geometric stiffness weakens the elastic stiffness to such an extent that stiffness is lost, instability phenomenons may occur, leading to a partial or a full collapse.

Since prestressing influences the stress state of the object, it may, in general, also influence its geometric stiffness, providing means to control the structural behaviour by fine-tuning its stiffness.

For example, a violin string is a prestressed object with much larger geometric stiffness than elastic hence its performance is primarily determined by the prestress. With violin

string cross-section area A, density ρ, length L, and constant tension T, the pitch or first natural frequency is, under the assumption of small displacements, determined as

$$f_\text{n} = \frac{1}{2L}\sqrt{\frac{T}{\rho A}},\tag{2.2}$$

and influenced by the musician in two ways. First, during tuning, the tension T is adjusted to obtain the desired pitch of the string; this introduces the correct level of prestress. Then, during the performance, the length L is adjusted by pressing fingertips against the string at different locations; pressing, for example, the fingertip halfway along result in a doubled pitch. As with the string, there is in more complex spatial structures a relation between prestressing and natural frequency which can be used to determine the state of stress in existing structures (Ashwear and Eriksson 2014).

Equation (2.2) originates from the partial differential equation describing the vibration mode at time t of the string

$$T\frac{\partial^2 y}{\partial x^2} - EI\frac{\partial^4 y}{\partial x^4} = \rho A\frac{\partial^2 y}{\partial t^2},\tag{2.3}$$

where y is the lateral displacement of the string at longitudinal position x and EI the elastic bending stiffness, which for a thin string is negligible compared to T.

Figure 2.2 depicts two cable-braced pin-jointed frames which could act as horizontal restraints in a building. The verticals and the horizontal are assumed sufficiently stiff not to buckle, whereas the diagonal cables buckle under compressive load. Structure (a) is not prestressed, so one cable buckles as P loads the structure, and the deflection δ_1 is determined primarily by the stiffness in the remaining tensioned cable; for small P, the elastic stiffness dominate, and with increasing P, the geometric stiffness increases casing a stiffening shown as a non-linear relation between P and δ_1. Structure (b) is prestressed using turnbuckles on the cables to such a degree that no cable buckles under load P, effectively doubling the elastic stiffness compared to (a) for the same amount of material; for small P, $\delta_2 \approx 0.5\delta_1$.

However, there are situations when the prestressing do not influence the stiffness at all. For example, the stiffness of a Bowden cable (see fig. 2.3), used to transmit force from the handle to the brakes on a bike, in surgery, robotics, et cetera, is determined only by the elastic stiffness of the sheeting and the cable. The reason is that the negative geometric stiffness in the compressed sheeting counteracts the positive geometric stiffness in the tensioned cable. While the geometric stiffness for the individual members may be substantial, the net effect on the entire system is zero.

2.1.4 Mechanics of bar frameworks, statically indeterminacy, and prestressing

A bar framework is a theoretical model of inextensible bars connected with friction-less joints that can model several structures such as trusses, tensegrities, cable nets, and approximate membrane-action dominated gridshells and, with a fine-enough resolution, continuous shells.
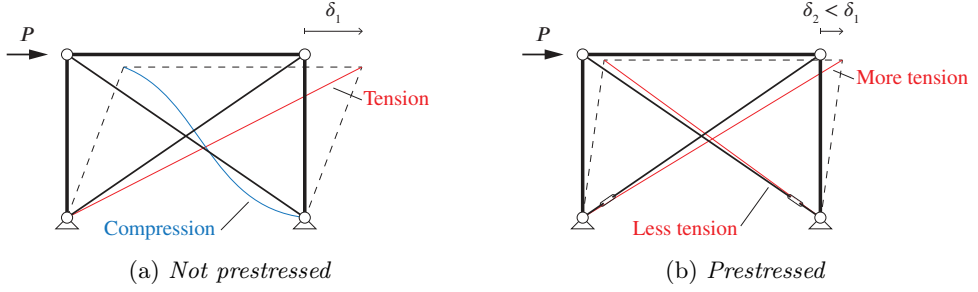
Figure 2.2: *Two cable-braced pin-jointed frames loaded with a horizontal load P causing the top node deflection δ. Both are equal except that structure (a) is not prestressed, whereas (b) is.*
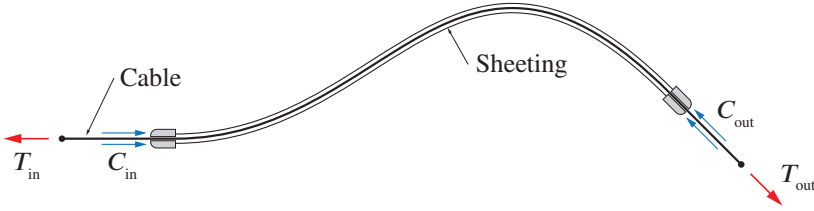
Figure 2.3: *Working principles of the Bowden cable. The forces applied on the cable corresponds to those applied on the sheeting. Due to friction between cable and sheeting, the input forces are slightly higher than the output forces.*

Initially presented by Möbius (1837) in an abstract format (Pellegrino 1986), there exists a simple condition for the rigidity of such bar frameworks, widely known as *Maxwell's rule* for the construction of rigid frameworks,

$$b - nj + c = 0, \tag{2.4}$$

where j is the number of joints, n the dimension of the space ($n = 2$ in two dimensions, $n = 3$ in three dimensions), b the number of bars, and c the number of kinematic constraints ($c \geq 3$ in two dimensions, $c \geq 6$ in three dimensions). If eq. (2.4) holds, the framework is statically determinate, whereas if the left-hand side is positive, it is statically indeterminate, and if negative, a mechanism.

However, just as Möbius, Maxwell (1864b) anticipated exceptions which the rule could not explain on its own. For example, one of Buckminster Fuller's tensegrity structures with 12 joints and 24 bars should, according to the rule, be loose with 6 degrees of freedom, yet it is stiff (Tibert 2002). More than a century later, Calladine (1978) presented an extended rule capable of dealing with all possible cases

$$b - nj + c = s - m, \tag{2.5}$$

where m is the number of internal mechanisms and s the number of states of self-stresses, or states of prestress. Equation (2.5) does not by itself solve m and s, numbers that

depend not only on the number of bars and joints and the topology but on the complete specification of the framework (Pellegrino and Calladine 1986). However, it introduces a clear explanation of the fundamental mechanics of bar frameworks.

The extended rule tells that, to prestress a bar framework ($s > 0$), it must be statically indeterminate ($b - 3j + c > 0$). Furthermore, there may be bar frameworks, such as Fuller's tensegrity structure ($m = 6$, $s = 6$), in which the induced prestress counteracts the mechanism, rendering the framework rigid. Figure 2.4 illustrates additional examples.

$b = 2$, $j = 3$, $c = 6$ $b = 3$, $j = 4$, $c = 9$ $b = 4$, $j = 5$, $c = 12$ $b = 3$, $j = 4$, $c = 9$
$m = 1$, $s = 0$ $m = 0$, $s = 0$ $m = 0$, $s = 1$ $m = 1$, $s = 1$

     (a)   (b)   (c)   (d)
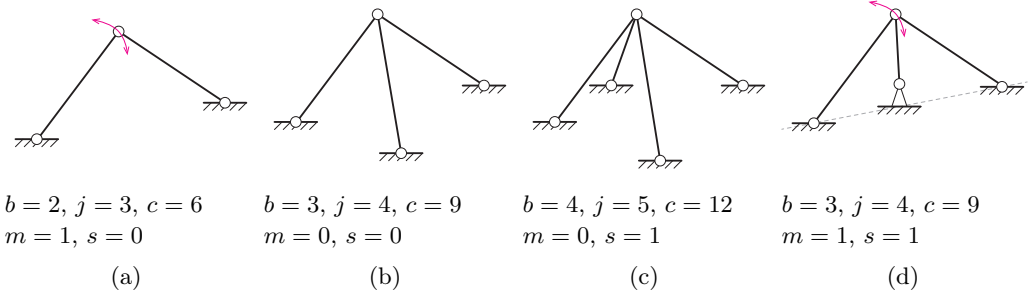
Figure 2.4: *Three-dimensional ($n = 3$) bar framework (a) is a mechanism that can freely rotate around the axis through the supports, (b) is a rigid statically determinate structure, (c) is a rigid statically indeterminate structure, and (d) a mechanism that, when activated, introduces a state of self-stress that counteracts the mechanism, rendering the structure rigid. In reality, none of the frameworks is rigid; the stiffness determines the resistance against deflection.*

2.2   Prestressing usage

Prestressing is applied virtually everywhere, to structures and everyday objects, by nature and humans, starting in prehistoric times. Although humans are arguably part of nature, it is convenient to discuss prestressing applied in nature and technics (technology; lending from Otto's *Pneus in Nature and Technics* (Bach 1977)) separately to highlight how humans have understood and used the concept. The following sections describe the application of prestressing and summarise the more extensive collection presented in the preceding licentiate thesis (Sehlström 2019).

2.2.1   In nature

Proteins are among the tiniest things prestressed in nature yet vital for life. The prestressed spectrin protein inside neurons enables the sensation of mechanical forces (Krieg, Dunn, and Goodman 2014), and studies on 'tensegrity-like pattern of prestress' in the protein ubiquitin may result in the creation of tailor-made proteins with mechanical properties for applications in medicine, material design, and nanotechnology (Edwards, Wagner, and Gräter 2012, p. 4).

Still small-sized, there is the turgor pressure in living cells which, similarly to a balloon filled with air, provides structural rigidity when the pressurised fluid contained by the cell stretches its wall. The turgor pressure can be as small as 0.1-0.4 MPa yet also exceed 2-3 MPa (a bike tire is around 0.2-0.6 MPa) and plays an essential role in processes such as growth, development, mechanical support, signaling, organ movement, flowering, and responses to stress (Beauzamy, Nakayama, and Boudaoud 2014; Luchsinger, Pedretti, and Reinhard 2004).

In trees, the turgor pressure is referred to as *growth stresses* and can be large enough to cause significant problems in the conversion of felled trees to timber (Wilkins 1986). The growth stresses are orthotropically distributed (Mattheck and Tesari 2004), its origin discussed by, for example, Münch (1938), Jacobs (1938), Kubler (1987), and Cassens and Serrano (2004), and explains why sawn timber deform (bow, crock, cup, twist). Due to the high risk of fibre buckling in wood (Boyd 1950), wood has a longitudinal compressive strength of only about half of its tensile strength. The growth stresses (fig. 2.5a) resist external forces, primarily from the wind (fig. 2.5b), and more even utilisation of the wood strength is obtained (fig. 2.5c), resulting in a much higher overall load-bearing capacity than if there were no prestresses present (Mattheck and Kubler 1995).

(a) *Growth stresses*   (b) *Bending stresses*   (c) *Resulting stresses*
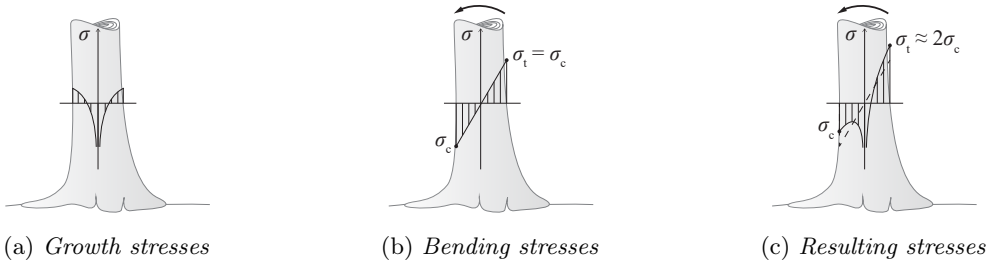
Figure 2.5: *Longitudinal stresses σ in a tree trunk. The growth stresses originate when wood cells in the outer part of the trunk contract in the longitudinal direction and expand in the transverse direction (Münch 1938), causing compression of the adjacent interior layers that reduce the tension of older cells (Jacobs 1938) leading to severe compression near the pith (Cassens and Serrano 2004).*

The longitudinal contraction is restrained by older cells, putting the new cells in tension (Kubler 1987), causing a compression of the adjacent interior layers that reduces the tension of older cells (Jacobs 1938) leading to severe compression near the pith (fig. 2.5a) (Cassens and Serrano 2004).

Some animals also prestress their structures. For instance, birds bend grass and branches as they build their nests, effectively inducing prestresses in the members that, with the help of friction, are restrained against one another and thus kept in place. Spiders prestress their webs to make them stiff enough to support the weight of themselves and their prey without substantial deflection using a minimum of material (Kullmann, Nachtigall, and Schurig 1975). The induced prestress also affects the sonic properties of the web, which transmits vibratory information to the spider; by alternating the tension, the spider can tune its web (Mortimer et al. 2016).

2.2.2 In technics

The following examples of prestressing applied within techncis are presented thematically in somewhat chronological order.

Early usage

Though impossible to date due to their simplicity, tents are likely the oldest example of prestressing applied by humans. Hide supported by slender branches bent into place, like in a bird's nest, is the assumed way of construction. With the invention of ropes and textiles, also requiring prestressing for their making, the tents developed further into portable, lightweight structures such as the yurt and tipi. In parallel, vessels for fishing and transportation were advanced with the help of prestressing, for example, skin boats, dating back at least 10 000 years, with a skin membrane wrapped and stretched around a timber frame (Evguenia 2016).

Reliefs depicting prestressed boats and barges in ancient Egypt are among the earliest records of advanced usage or prestressing, dating back to c. 2700 BCE (Leonhardt 1964). A system of entwined ropes from stern to bow, prestressed by additional twisting, prevented the vessels from hogging, keeping the deck in level (Torr 1895; Casson 1971). The mightiest is perhaps the barge depicted on the wall of Queen Hatshepsut's temple in Dar el-Bahri (fig. 2.6).

A stretched string loses its prestress as soon it is released from its anvil, minimising its stored strain energy. Bows, developed for hunting and warfare, leading to the medieval English longbow with a range of up to 315 m (Oakeshott 1960), utilise this phenomenon, and later also catapults (Gordon 1978). The tensioning of the bowstring stores strain energy in the bow, further increased by the archer pulling the string backward, which, upon release, rapidly accelerate the arrow forward. Similar things happen in sports rackets (Kullmann, Nachtigall, and Schurig 1975) where kinetic energy in the ball and racket at impact converts to strain energy, deforming the ball and the net. But the deformed state is not minimal, so the ball and net try to get back to a lower energy state, converting strain energy back into kinetic energy, forcing the ball to spring off the net, which returns to its initial flat configuration. Of course, some energy dissipates during these processes as thermal energy and air movements. For the bow and racket, the dissipation is unwanted, reducing the kinetic energy in the arrow or ball, whereas desired in string instruments, which are prestressed so that the strain energy dissipates as sound waves as it oscillates with decreasing amplitude in a precise manner until reaching its initial configuration, giving rise to tones while playing.

Stone and masonry

The Romans controlled the stress trajectories within masonry by prestressing (Todisco 2016), effectively fine-tuning the structure's weight. For example, the attic of the Colosseum (70–80 CE) in Rome adds extra weight in the upper part that compresses the lower, counteracting tensile stresses at the base caused by wind. In the Pantheon (118–128 CE) in Rome, the varying density of the concrete help steers the thrust towards the foundation.
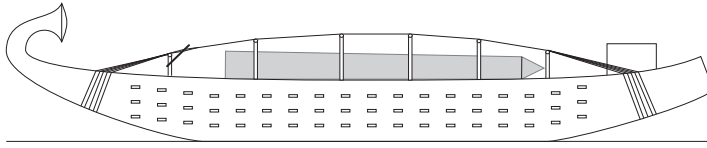
Figure 2.6: *Hatshepsut's barge c. 1470 BCE. Loaded with two obelisks, each weighing around 375 t, it was towed on the river Nile from the quarry in Aswan 213 km to the temple in Karnak.*
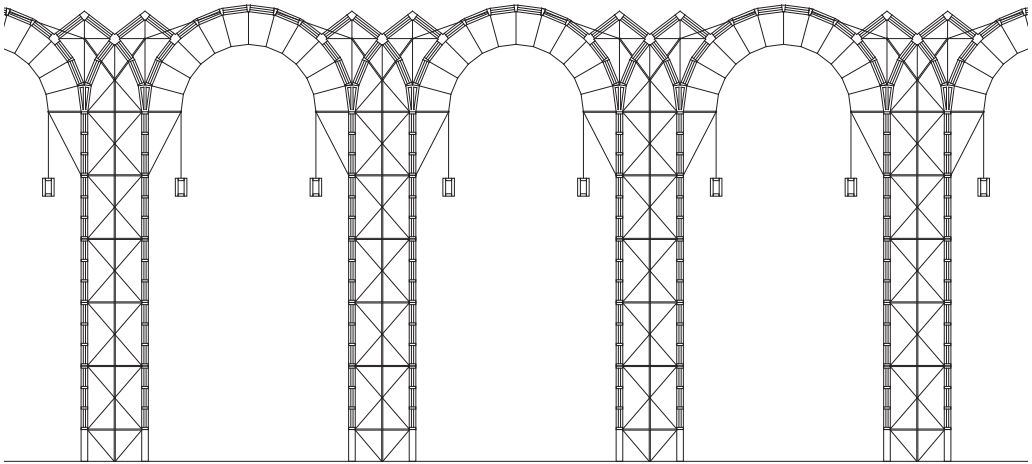
Figure 2.7: *Elevation of parts of the façade of Pavilion of the Future (1992) in Seville, Spain*

(a) *Before installation of wedges*

(b) *After installation of wedges*

Figure 2.8: *Laminated timber beams using wedges and metal wraps*
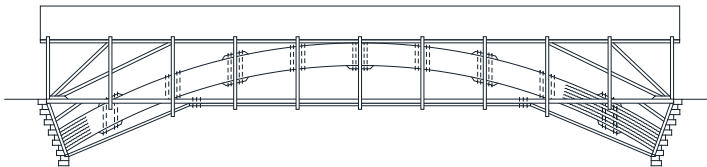
Figure 2.9: *Wettingen brücke (1765) by brothers Johannes and Hans Ulrich Grubenmann. The timber bridge, which crossed the Limmat River in Switzerland, was burned by French troops only a few decades after its completion during the French Revolutionary Wars.*

15

During the medieval period, refinements of the technique enabled the construction of Gothic cathedrals, where pinnacles add weight to steer thrusts in the flying buttresses down into the buttresses (Addis 2007).

Heyman (1966) provides a rigorous framework of limit state analysis applied to masonry structures, stating that the masonry is safe if the thrust line representing the path of the compressive resultants of the stresses lies within the cross-section for all possible load cases. The measures undertaken by the Romans and medieval master builders effectively controlled the path of the thrust line.

More recently, Peter Rice controlled the thrust line in the Pavilion of the Future (1992) in Seville, Spain (fig. 2.7) using a series of tie-rods to lift the weight of an adjacent roof and apply it radially to the stone arches of the façade (Addis 1994; Lenczner 1994; Rice 1996).

Timber

Traditional timber structures contain several examples of prestressing, enabling short members to be assembled effectively, allowing longer and taller constructions (James 1982). The development of the joints follow closely with the development of suitable tools (Zwerger 2000).

Several traditional timber joints rely on wedges (Krauth and Meyer 1893, fig. 59), which, when driven in between the members, pushes them apart and locks the connection through friction and a normal force. Wedges in combination with iron straps (fig. 2.8) enabled the Swiss Grubenmann family (Brunner 1921; Brunner 1924; James 1982; Killer 1942; Weinand 2016) to construct the first curved laminated timber arches, leading to the construction of the Wettingen bridge in 1765 (fig. 2.9; S. Samuelsson 2015). The bridge aroused the admiration of their contemporaries almost immediately and was, partly due to the explosion of architectural research, travel, and publication starting in the 1750s (Bergdoll 2000), already widely known in 1770 (Angelo and Maggi 2003). Recent studies provide insights on the design and analysis of laminated arches (Miller 2009).

The rapid expansion of the U.S. railway led to the further development of prestressed timber bridges during the 19th century. It began with a patent by Long (1830) for a timber truss bridge in which 'counterbraces' were put in compression using wedges, see fig. 2.10, hence avoiding tension connections (Gasparini and Provost 1989; Gasparini and Simmons 1997; Gasparini and Porto 2003). The patent introduced mathematical principles of engineering (Christianson and Marston 2015). Long filed for further patents (Long 1839) and was recognised by contemporary Carl Culmann (1851), but his inventions were soon made obsolete (Sutherland 1997) as new patents by Howe (1840), see fig. 2.11, and T. W. Pratt and C. Pratt (1844), see fig. 2.12, introduced pre-tensioned iron rods into trusses.

Today, the development and usage of prestressed timber focus primarily on on post-tensioned engineered timber members and structures, for example, beams with internal steel tendons (D'Aveni and D'Agata 2017) and external steel plates (McConnell, McPolin, and Taylor 2014), stress-laminated decks (Oliva et al. 1990; Ekholm 2013), and frames with tendons passing through members and joints, creating moment stiff connections (Palermo et al. 2005; Granello et al. 2018; Buchanan, Deam, et al. 2008; Newcombe

Figure 2.10: *Longs's 1830 patent (Long 1830)*

Figure 2.11: *Howe's 1840 patent (Howe 1840)*

Figure 2.12: *Thomas and Caleb Pratt's 1844 patent (T. W. Pratt and C. Pratt 1844)*
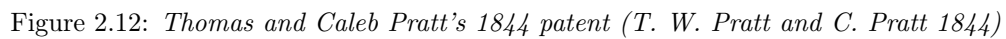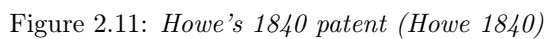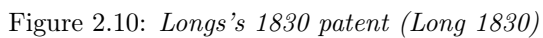
2011; Buchanan, Palermo, et al. 2011; Curtain et al. 2012; Wanninger and Frangi 2016; Wanninger 2015) with favourable seismic behaviour (Wanninger and Frangi 2014).

Concrete

Reinforced concrete is the most widely used construction material today. It is a mouldable material with high compressive strength. But it has a brittle failure even at very low tensile stresses, hence the added reinforcement, ensuring a ductile behaviour with plastic failure at much higher stress levels. In addition, concrete shrinks and creeps over time, altering its material properties. These issues triggered investigations that led to the development of prestressed concrete during the late 19th and early 20th centuries.

The general idea of prestressed concrete is to compress the concrete section to partially or fully avoid tensile stresses (e.g. due to self weight and external loading) within the concrete, resulting in uncracked concrete with higher flexural capacity, increased corrosion resistance, and better liquid-containing properties than cracked reinforced concrete. Furthermore, prestressing improves the shear resistance and allows reduced cross-sections, resulting in material and cost savings (Kaylor 1961).

Leonhardt (1964), Menn (1990), and Sanabra-Loewe and Capellà-Llovera (2014) covers the history of prestressed concrete in broad terms, Hellström, Granholm, and Wästerlund (1958), Haegermann, Huberti, and Möll (1964), and Engström (2011) provide additional details. A brief summary follows. Preceded by at least three patents applying prestressing to building construction, Jackson (1886) received the first patent on prestressed concrete using tie-rods to compress the concrete. It was followed by several patents by others over the next coming four decades, for example, one by the Norwegian Jens Lund (1912), however few of these systems had any practical application. Only when the French engineer Eugène Freyssinet (1879–1962) recognised the full potential, the concept became applicable at a large scale. His work and observations on how to control creep, then a little-known phenomenon, led to several patents in 1928, stressing the importance of full prestressing, a design philosophy prevailing until the late 1960s when partial prestressing took over.

In parallel with Freyssinet, Spanish engineer and researcher Eduardo Torroja (1899–1961) took an interest in prestressed concrete (Sutherland 2001; Ochsendorf and Antuña 2003), resulting in the 1925 Tempul (Torroja 1962; Lozano-Galant and Paya-Zaforteza 2017) and the 1939 Alloz (Torroja 1948) aqueducts, the latter discussed in detail in Paper F. Torroja co-founded in 1949 the Spanish Prestressed Concrete Association, in 1952 the Féderation Internationale de la Précontrainte (FIP), and in 1953 the Comité Européen du Béton (CEB) (Corres and Leon 2012); later, in 1998, FIP and CEB merged into the International Federation for Structural Concrete *fib*.

Prestressed concrete is either post-tensioned, commonly used for in situ concrete, or pre-tensioned, commonly used for prefabricated members; in the former case, steel tendon tensioning takes place after (post) concrete curing, whereas in the latter, before (pre). In either case, strain compatibility between the concrete and the steel and substantial differences in cross-section area and modulus of elasticity necessitate the need to use high-strength steel tendons when prestressing concrete. Two major systems for post-tensioning concrete dominate the market: the Freyssinet system, with steel strands locked using

wedges, and the Macalloy system, with threaded bars and bolts to lock the system, see fig. 2.13. Both use hydraulic jacks to tension the steel tendon, which runs in ducts, either filled with cement grout after anchorage to get a continuous bond between steel and concrete or with grease for an unbonded design. When pre-tensioning, steel strands are tensioned between two anvils so that the strands run through the casting mould. Then the concrete is cast, encapsulating the strands, and cured for some time before releasing the strands from their anvils, effectively relaxing some of the tension in the strands and compressing the concrete.
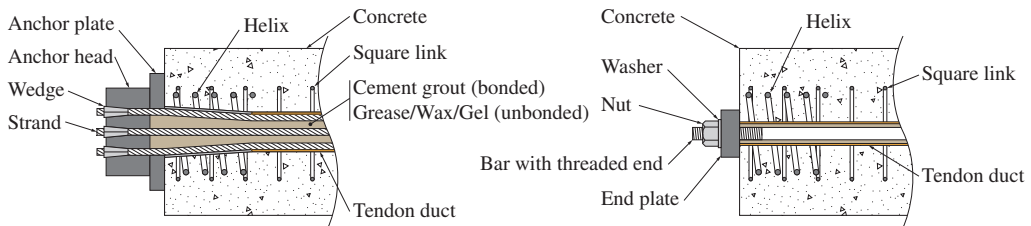
Figure 2.13: *Typical design of concrete post-tensioning anchors. The Freyssinet system to the left and the Macalloy system to the right. The longitudinal compressive stresses in the concrete give rise to transverse tensile stresses, taken care of by the mild reinforcement steel helix and square links surrounding the duct.*

Currently, there is an interest in using other tensioned materials than steel, such as carbon-fibre-reinforced polymers, to compress the concrete, both in new construction and for strengthening existing ageing concrete structures. The application can lead to increased elastic bending stiffness, smaller crack openings, and increased ultimate capacity (Yang 2019).

Wheels and restrained arches

Prestressing has been used for a long time to construct lightweight wheels. Early construction relied on wet rawhide placed on the exterior of the rim that dried and shrunk, binding the hub, spokes, and rim segments together. Later, when iron became readily available, the wheels were fitted with an iron hoop or streaked with iron, compressing the woodwork and protecting against wear (fig. 2.14). The methods have similarities with those used to make wooden barrels bound by metal hoops.

The first prestressed iron Ferris wheel was built by George Washington Gale Ferris Jr. for the World Columbian Exposition in Chicago 1893. The 76 m wheel carried 36 cars and had an outer layer of bars prestressed by an inner layer of post-tensioned cable spokes, see fig. 2.15a. The wheel no longer exists, but the similar 1897 Wiener Riesenrad in Vienna, Austria still operates (Kullmann, Nachtigall, and Schurig 1975). Until this point, designers understood the prestressing concept sufficiently and applied it 'effectively and safely, albeit without analyses based on structural mechanics' (Gasparini, Bruckner, and Porto 2006, p. 418). Ferris' wheel changed this, and J. B. Johnson, Turneaure, and Bryan (1894) provides an early and realistic mathematical model for the analysis of the effects of prestressing, live load, and their sum in the context of a Ferris wheel, see fig. 2.15.

Figure 2.14: *Two methods of shoeing a wheel. In the centre the labourers are using hammers and 'devils' to fit a hoop onto the rim, and on the right they're hammering strakes into place.*

Originally published by Diderot and Rond d'Alembert (1769)

Today, many Ferris wheels, such as the High Roller and London Eye (Engström et al. 2004), have pretensioned spokes aligned along a narrow compressed rim and a wide hub, just as modern bicycle wheels. Then the inclined spokes provide some elastic stiffness and substantial geometric stiffness so that the wheel better withstands lateral forces in addition to the radial (Brandt 1993). Similar cable-restrained circles formed the substructure for the hull of Zeppelins (Kullmann, Nachtigall, and Schurig 1975, p. 143).

Pre-stressed cables are also used to restrain arches. The glass roof of the Moscow GUM department store (1890–1893) and the Pushkin Museum (1898–1912), both by lightweight-shell pioneer Vladimir Shukhov (1853–1939) (Wells 2010), are stiffened by cables springing from the ends connecting once to the arch (Graefe and Tomlow 1990). Eugene Freyssinet used the same topology for the formwork for the 1923 Orly airship hangar (Frampton and Futagawa 1983; Frampton 2007), see fig. 2.16a. More recently, Peter Rice let, for the glass roof of the bus terminal in Chur, Switzerland (1988), all cables radiate towards the roof arch from a central nave located just above the focal point of the arch (Rice 1996; Addis 1994). Jörg Schlaich used the same principle in 1989 for the glass roof at the Museum of Hamburg History (Barkhofen and Bögle 2010) and again in 1998 for the glass roof at the DZ-Bank in Berlin (J. Schlaich, Schober, and Helbig 2001). Other examples include the Japan Pavilion at Expo 2000, where Shigeru Ban, who collaborated

(a) *Ferris wheel*

(b) *Prestress*

(c) *Loading*

(d) *Result*
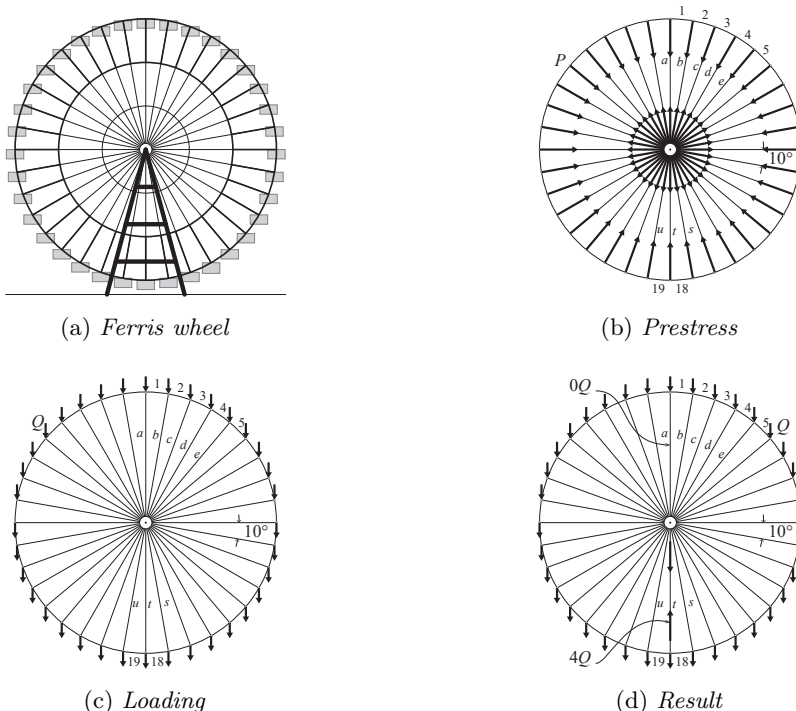
Figure 2.15: *Illustration of Ferris' wheel (1893) and load analysis according to J. B. Johnson, Turneaure, and Bryan (1894). Under linear relations and by superposition of load cases and a symmetry argument, the prestressing force P in each cable (b) has to be twice the weight of each car Q (c), i.e. $P = 2Q$. Then there will be 0 force in cable* a *and the maximum tensile force $4Q$ in cable* t *(d), compared to the case without prestressing, where non-buckling bars replace the cables, resulting in a maximum compression force of $5.68Q$ in bar* a *and maximum tensile of $11.48Q$ in bar* t.

(a) *Orly Hangar*

(b) *Japan Pavilion*

(c) *Berlin Hauptbahnhof*
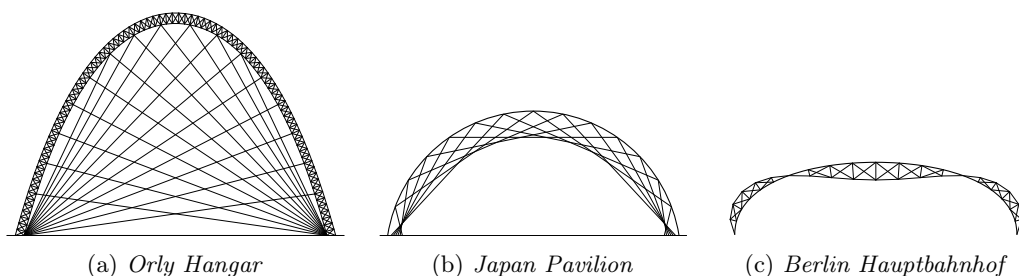
Figure 2.16: *Cable-retrained arches (not to scale)*

with Frei Otto on the project, let the cables spring from the ends and connect multiple times to the arches (Ban 2000), see fig. 2.16b. There is also the shallow glass roof of Berlin Hauptbahnof (2006), where Schlaich has let the cables trace the tension side of the moment diagram of the arches, leaving the space below clear (Detail 2005; Falk and Buelow 2009), see fig. 2.16c. The degree of prestress in these systems is low, with enough tensile stress to make sure that the cables never run slack which would cause them to lose their stiffness completely. Such a loss would lead to an increase in the buckling length of the arch, making it more susceptible to instability phenomenons.

Swiss engineer Jürg Conzett illustrates another way to restrain an arch in his Wasserfallbrücke (2003) in Flims, Switzerland (Dechau 2013). The bridge consists of a thin masonry arch compressed and stiffened by post-tensioned steel plates placed on top, leading, just as for the Pavilion of the Future (fig. 2.7), to a radially uniformly distributed force, effectively ensuring the thrust line lies within the stone section, see fig. 2.17a. Similar solutions, but with internal tendons running through the masonry, are found in the stone arches supporting the roof of Padre Pio Pilgrimage Church (2004) in San Giovanni Rotondo, Italy (Rice 1996), and in the prototype bridge made of re-used concrete blocks (2021) by the Structural Exploration Lab at EPFL (Fivet 2021), see fig. 2.17b.

(a) *Wasserfallbrücke (2003)*   (b) *Bridge made of re-used concrete (2021)*

Figure 2.17: *Post-tensioned masonry bridges*
Image (b) courtesy of Corentin Fivet at Structural Xploration Lab

Pneumatic structures

Beginning in the 1960s, Frei Otto explored the potential of pneumatic structures, leading to several IL publications (Bubner 1975; Bach 1977; Drüsedau 1983; Otto and Rasch 1995). Expo '70 in Osaka exhibited various pioneering pneumatic buildings, but since then, no substantial development has been made other than the use of the airhouse to cover tennis courts and large sports arenas (Luchsinger, Pedretti, and Reinhard 2004). Pneumatic structures are, however, often used as components of building envelopes, such as the ETFE foil cushions used at the Eden Project (2001) in the UK, the Beijing Olympic Aquatics Centre (2007), and Roof Annex Lutherhaus (2010) in Germany (Liu, Zwingmann, and M. Schlaich 2015). In the latter, air-filled cushions suspend between cable-supported circular steel beams, see fig. 2.18.

Pneumatic structures, or *pneus* as Otto called them (Fabricius 2016, p. 1264), can also

be used as lightweight load-bearing components (Otto 1995) such as beams or bridges as exemplified by Luchsinger, Pedretti, and Reinhard (2004), Pedretti and Luscher (2007), and Zieta, Dohmen, and Teutsch (2008).

Figure 2.18: *Lutherhaus, Germany (2010). Pressurised transparent foil cushions suspended between cable-supported steel beams.*

Copyright Schlaich Bergermann Partner. Reproduced with permission.

Cable nets

Cable nets efficiently carry loads by tension and are often prestressed to limit their deflection under loading, and have been used for a long time to cover large areas. For instance, evidence suggests (Krizmanić 2020) the Colosseum (70–80 CE) in Rome and other contemporary amphitheatres had a *velarium* consisting of ropes supporting retractable textiles covering the stands.

However, substantial advancements of cable net roof structures took until the 1950s (Krishna and Godbole 2013), beginning with the Dorton arena (1953) in Raleigh, U.S. (Otto 1954), see fig. 2.19. Several roofs followed in the coming decades (Kullmann, Nachtigall, and Schurig 1975), such as Scandinavium (1971) in Göteborg, Sweden (Kärrholm and A. Samuelsson 1972). Frei Otto's work led to the design of Olympiastadion (1972) in Munich, Germany (Tomlow 2016), see fig. 2.20. On the design team, among others such as Fritz Leonhardt, John Hadji Argyris, and Klaus Linkwitz, was Jörg Schlaich, who since then through his practice has contributed to the development of prestressed cable net structures (M. Schlaich 2018).

Most cable nets are anticlastic (curved in two opposite ways; saddle-shaped), being, in general, stiffer than flat nets. As a consequence, flat nets require higher levels of prestress to compensate, resulting in large support structures, which is the case for the cable-net-supported glass façade of the Hilton Hotel (1993) at Munich Airport (Schober and Schneider 2004; Barkhofen and Bögle 2010).
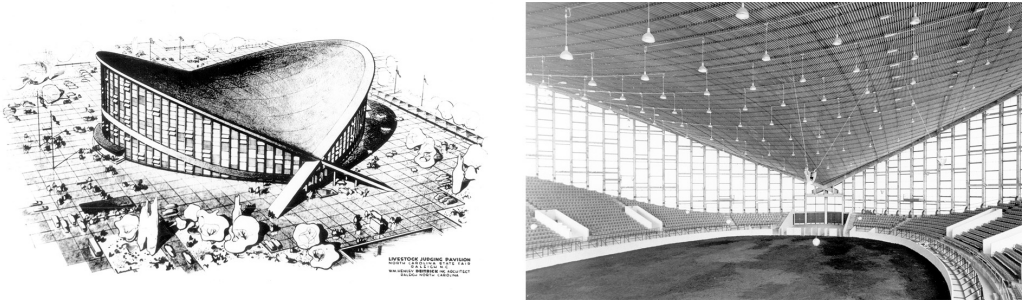
Figure 2.19: *Dorton arena (1953). Drawing (left) and view of the cable net roof from the inside (right).*
Images courtesy of the N.C. State Fairgrounds

Figure 2.20: *Olympiastadion (1972) in Munich by Frei Otto, Jörg Schlaich, Rudolf Bergermann, et al*
Image by Taxiarchos228, Munich: Olympic Stadium, 2016-08-01. de.wikipedia.org. Copyleft: This is a free work, you can copy, distribute, and modify it under the terms of the Free Art License artlibre.org/licence/lal/en

Tensegrity

Tensegrity structures offer perhaps the most sophisticated use of prestressing, which through a clear distinction between pin-jointed compression and tension members (Wroldsen 2007) gain a high mechanical efficiency (Ashwear 2016). While the word *tensegrity*, which is a contraction of *tens*ile and int*egrity*, was coined by Buckminster Fuller (1895–

1983) in a patent (Fuller 1962), there is a dispute regarding the true inventor and the origins of the idea (Snelson 2012), but the sculpture *X-Piece* (1948) by artist Kenneth Snelson (1927–2016) is generally regarded as the birth of the tensegrity concept (Tibert 2002). For a more extensive exploration of the origins of the concept, see the series of articles and responses in the special issue of *International Journal of Space Structures* (Lalvani 1996).

There exists several variations of the definition of the concept, see, for example, Fuller (1962), Pugh (1976), Hanaor (1994), Skelton et al. (2001), and Motro and Raducanu (2003). Miura and Pellegrino interpret a tensegrity structure as 'any structure realised from cables and struts, to which *a state of prestress is imposed that imparts tension to all cables*' and adds that 'as well as imparting tension to all cables, the state of prestress serves the purpose of *stabilising the structure*, thus providing first-order stiffness to its infinitesimal mechanisms' (Tibert 2002; Tibert and Pellegrino 2003). Many definitions limit the allowable element types to struts and ties. However, relying on Fuller's more poetic definition of tensegrity as 'islands of compression in a sea of tension' (Safaei 2012), one could argue that other kinds of element are possible to use in a tensegrity structure (Motro and Raducanu 2003), such as continuous fabric stretched against discontinuous struts.

Snelson exhibited many tensegrity artworks, several depicted in his book (Snelson 2013), and Robert Le Ricolais (1894–1977) applied principles of tensegrity in his explorations of spatial structures (Nsugbe and Williams 1999; Motro 2007). Cecil Balmond used the concept in 2006 for his *H_Edge* structure (Balmond 2007). In 2003, Snelson's record of highest tensegrity structure was ousted by the 62.3 m tensegrity tower in Rostock, Germany, relying on pre-tension forces up to 1100 kN for its rigidity (M. Schlaich 2004). But the tensegrity concept has proven difficult to implement in its pure form within architecture and civil engineering (M. Schlaich 2004). However, some structures have tensegrity-like features, such as large domes, temporary structures, tents (Safaei 2012), and stadium roofs but also glass façades and roofs (cf. section 2.2.2). Both Olympiastadion in Munich (fig. 2.20) and the Millennium Dome from 1999 (fig. 2.21) by Richard Rogers and Buro Happold (Liddell and Westbury 1999), with their tensile membranes, cables, and so-called flying masts (Wroldsen 2007), are examples. The concept has also inspired bridge designs, such as the Royal Victoria Dock Bridge (1998) in London by Techniker and Lifschutz Davidson and the Kurilpa Bridge (2009) in Brisbane, Australia by Ove Arup & Partners.

Rice Francis Ritchie (RFR) (Rice 1996), during the 1980s considered the best engineering firm in glassed tensed structures worldwide (S. Samuelsson 2015), designed façades with tensegrity features. With the Glass Walls (Les Serres) at the Parc de la Villette, Paris (1982–1986) in their portfolio (Patterson 2011), RFR were consulted for the design of the Grand Pyramid (1989) and the Inverted Pyramid (1993) at the Louvre in Paris (fig. 2.22). Architect Ieoh Ming Pei (1917–2019) asked the engineers to create a 'structure as transparent as technology could reach' (Knoll 1989; NCK n.d.). The Grand Pyramid consists of steel beams stiffened by post-tensioned steel cables and compression struts. These are placed in two directions parallel to the pyramid edges to support the glass panels and handle the wind pressure. Several horizontal cable rings redistribute suction forces due to wind from one side of the pyramid to the opposite (Engström et al.

2004). The Inverted Pyramid takes advantage of structural glass and post-tensioned rods, rendering the need for a supporting frame unnecessary.

Figure 2.21: *Millennium Dome, London, UK (1999) by Richard Rogers and Buro Happold*
Image by James Jin (2004); CC BY-SA 2.0 license; cropped;
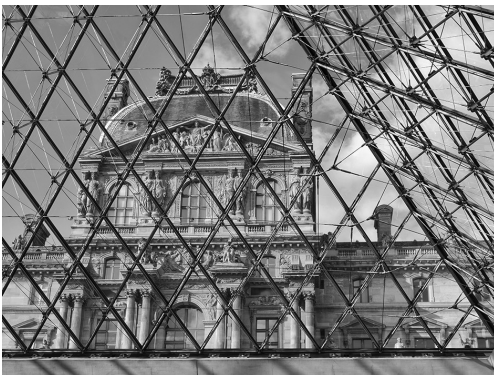*flickr.com/photos/44768990@N00/58712717*

Figure 2.22: *Grand Pyramid (1989; left) and Inverted Pyramid (1993; right) at the Louvre, Paris*

Left image by Babyaimeesmom (2018); CC BY-SA 4.0 licence; cropped, made black & white; commons.wikimedia.org/wiki/File:Louvre_Palace.jpg. Right image by Lucas Lima (2017); CC BY-SA 2.0 licence; cropped; flickr.com/photos/lucasnave/34167423466

2.3 Active and inactive prestress

Among the presented examples in section 2.2, two types of prestress are distinguishable: *active prestress* and *inactive prestress*.

Active prestress affects the global state of stress and links to Maxwell's rule requiring a bar framework to be statically indeterminate to prestress it.

Inactive prestress only affects the local state of stress. Think, for example, of a simple column (fig. 2.23b). It is statically determinate, and, by the logic of Maxwell's rule, it cannot be prestressed. However, if replaced by a cable-stiffened post (fig. 2.23c), it can indeed be prestressed by tensioning the cables. Yet, the overall state of stress is still statically determinate, and the net effect of the prestress is virtually zero, no matter how much the cable is tensioned (until the cable snaps or the post buckles). The same applies to the cable-restrained arches in fig. 2.16. Wu and Sasaki (2007) discusses the structural behaviours of an arch stiffened by cables, concluding that the 'natural frequencies and the damping ratios ... change little when two kinds of pre-tension ($49\,\mathrm{N}$ and $147\,\mathrm{N}$) are introduced.' Thus, the level of pretension does not affect the behaviour in any significant way, as long as it is enough to keep the cables tensioned.

(a) *Arbitrary structure*   (b) *Column, $C_0 = P$*   (c) *Cable-stiffened post, $C_1 \neq P$*
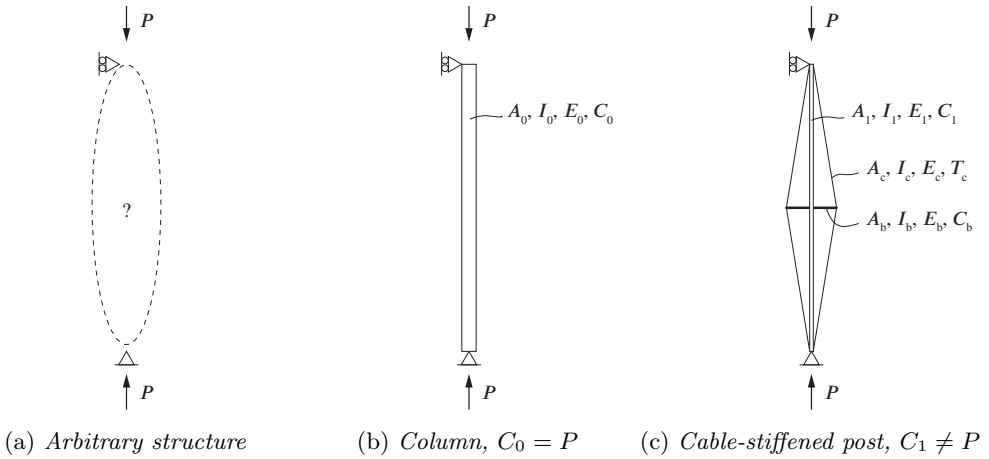
Figure 2.23: *Simply supported globally statically determinate structures. Regardless of the structure placed between the supports, the applied load and the reaction are statically determinate and equal, and none can be actively prestressed, only inactively. Although the cable-stiffened post is compressed as the cables are pretensioned, it requires in general less material than the column ($A_1 < A_0$) to withstand the same load P since the buckling length of the post is reduced by the stiffening cable system.*

However, inactive prestress may still result in improvements in terms of increased material efficiency compared to using ordinary columns or beams, such as the cable-supported beams in the Louvre Grand Pyramid (fig. 2.22) and at Lutherhaus (fig. 2.18) and the cable braced lattice of The Symbolic Globe (1995) by Erik Reitzel (1941–2012).

2.4 Prestressing objectives and strategies

The presented examples in section 2.2 represent only a selection of all possible applications of prestressing, but the collection is large enough to classify and identify generalities. The licentiate thesis (Sehlström 2019) preceding this dissertation describes the details of the classification, including history, behaviour (material, member action, structural action), analysis and design approaches, the reason for prestressing, and its realisation. Although 'arbitrary and rough,' the classification may 'be useful as a help for understanding and discussions, if its imperfections and incompleteness are borne in mind' (Arup 1985, p. 34). The work resulted in the proposition of general prestressing objectives and strategies. These have been further developed and the result is summarised in table 2.1 and table 2.2 respectively.

The suggested objectives in table 2.1 help clarify what it means to *improve the performance* of the prestressed object. Several objectives can apply to the same structure, and there are unequivocally additional objectives than those suggested. Still, the suggested objectives have value, where the incompleteness and inconstancy of the list facilitate further discussion, perhaps provoking the formation of new perspectives offering means for deepened understanding.

The strategies in table 2.2 depart from how the prestressing is balanced, either as an externally equilibrated or auto-equilibrated system. Which of the two is, to a large extent, defined by the system boundaries. Consider, for example, a spiderweb and the roof of the Scandinavium arena. The structures are very similar, with multiple tensioned threads or cables. Despite this, the spiderweb is externally equilibrated, whereas the roof is auto-equilibrated. The argument for this is that the spiderweb gives rise to tensile reaction forces at the points where it is attached to surrounding objects proportional to the prestress in the web, whereas the tension in the roof cables are balanced by compression and bending in the surrounding edge beam, and the level of prestressing do not affect the reaction forces at all. But if the edge beam is considered external to the roof structure, it would no longer be auto-equilibrated but externally equilibrated, just as the spiderweb.

Table 2.1: Objectives with prestressing

---
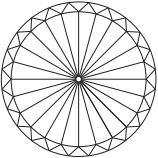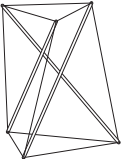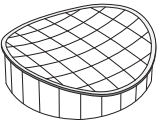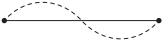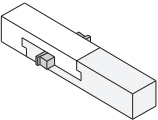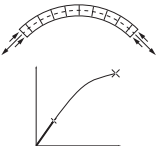
1 Stiffness

1a Obtain material efficiency

Prestressing to avoid compression/buckling:
Ferries wheel, cable roofs, growth stresses

1b Ensure stability

Prestressing to provide positive geometric stiffness and remove internal mechanisms:
Tensegrities

1c Provide form stability

Prestressing to maintain geometry:
Tensile membranes, pneumatic structures, Ferris Wheel & bicycle wheel, spiderweb, Egyptian barges, cables for formwork for Orly hangar, cable roofs

1d Obtain frequency

Prestressing to tune (often slender) members to a specific frequency:
String instruments, bicycle spokes (during truing of wheel)

---

2 Strength

2a Construct efficient joinery

Prestressing to secure connections (avoid tension in joints):
Masonry structures, traditional timber joints, modern bolted joints, birds nest

2b Achieve ductile behaviour

Prestressing to use material ductile stress-strain behaviour:
Masonry, concrete

Prestressing to achieve global ductility:
Pres-lam/Flexframe, Padre Pio Pilgrimage Church

2c Store energy

Prestressing to store strain energy:
Bow, racket & sports equipment

Table 2.2: Strategies for prestressing

1 Externally-equilibrated system

Inner forces balanced by reaction forces at boundary; prestressing increases reaction forces

1a Tensile reaction forces

Inner stresses balanced by tensile reactions:
Spiderweb, Hilton hotel at Munich Airport

1b Compressive reaction fores

Inner stresses balanced by compressive reactions:
Gothic Cathedrals & timber buildings with heavy roofs

1c Mixed reaction fores

Inner stresses balanced by both *tensile and compressive reactions:*
Suspension bridges, cable-stayed radio masts

2 Auto-equilibrated system

Tension and compression internally in balance; prestressing do not affect reaction forces

2a Inflation

Membrane in tension enclosing compressed fluid:
Pneu & turgor pressure, airhouse & ETFE cushions

2b Active bending

Prestressing by active bending, usually restrained by string or membrane in tension:
Birds nest, bow, tents & skin on frame boat, hull of Egyptian barges

2c Aligned tension/compression

Tension and compression member along a mutual line of action:
Prestressed concrete beam, Pres-lam/Flexframe, Wasserfallbrücke & Padre Pio Pilgrimage Church

2d Distributed tension/compression

Tension and compression members along individual lines of actions:
Egyptian barges, string instruments & racket, cable roofs & nets, restrained arches & wheels, tensegrities

2e Local prestressing

Pushing parts away/together:
Timber joinery with wedges

3 Shell structures

This chapter begins with a brief discussion on different types of shells in section 3.1. Then it introduces differential geometry in section 3.2 used to describe the curved geometry of shells and points out some curvature-related properties. Eventually, this enables the formulation of basic equilibrium equations in section 3.3. Following the maths-intensive sections 3.2 and 3.3, the Airy stress function is discussed in section 3.4 along with means to help deal with the interplay between geometry and stresses in membrane-action shells.

3.1 Types of shell structures

Continuous shells in concrete or steel primarily carry compression and occasionally also tension. Commonly, bending stiffness is provided to avoid buckling by, for example, adding stiffening ribs to a concrete shell as exemplified by Nervi (1956) or using corrugation as discussed by Thompson (1942). If the shell have unsupported edges and have too little bending capacity, it may be necessary to reinforce the edges, for example, with stiffening lips, as in the Wyss garden concrete shell by Heinz Isler (1926–2009), see fig. 3.1a, or edge beams, possibly prestressed as in Smithfield Poultry Market (Trout 2020, p. 523), see fig. 3.1b.

(a) *Wyss garden concrete shell in Zuchwil (1962) by Heinz Isler*

(b) *Smithfield Poultry Market in London (1963) by Ove Arup & Partners and Ronald Jenkins*

Figure 3.1: *Concrete shells with reinforced edges*

Image (a) by Chriusha – Own work; CC BY-SA 3.0 licence; commons.wikimedia.org/w/index.php?curid=7673963 and (b) by Phillip Perry; CC BY-SA 2.0 licence; cropped; commons.wikimedia.org/w/index.php?curid=5068208

Masonry shells—or vaults—can contain only compressive stresses since the bed joints of masonry have virtually no tensile strength. For vaults to stand with negligible tensile capacity, they must have 'a good structural shape' (Block 2009). Masonry has a high ratio between compressive strength and weight, and with a funicular shape, they can, in theory, be made very thin before crushing of the masonry occurs. However, the strength of masonry is generally not decisive for the design. Instead, it is the stability of the

structure, and so the vault must be proportioned based on stability (Heyman 1966). The instabilities may be caused by differential foundation settlements, earthquakes, long-term deformations (Block 2009), imperfections, and, for thin or long-span masonry, varying live-loads. The instabilities cause a bending action, making the vault behave more like an arch, and the movement of the line of thrust provides means to carry the bending. Heyman (1966) applies plasticity theory to masonry vaults and assumes the masonry is safe as long as it can contain all possible lines of thrust. Block and Ochsendorf (2007) extends the concept of the two-dimensional thrust line to a three-dimensional network of thrust lines which the structure must contain within itself. Thus, taking into account stability during design necessitate a certain thickness of the vault, which may not have to be constant (Rippmann, Van Mele, et al. 2016).

Gridshells consists of a grid of load-bearing laths made of, for example, timber, steel, or carbon fiber reinforced polymers. All shells must have bending stiffness to resist buckling and inextensional deformation (Adriaenssens et al. 2014, p. 26) due to point loads and uneven loading. This is particularly important for gridshells, and Adriaenssens et al. (2014, p. 243) conclude that 'a gridshell with pinned connections should never be built.' The bending stiffness provides the capacity to transfer bending moments out of the plane. It can be added to gridshells using, for instance, several connected layers of continuous laths as in Multihalle Mannheim (Happold and Liddell 1975; Vrachliotis 2017) or sufficient member height and bending stiff joints as in the British Museum Great Court Roof (Williams 2001).

If the shell contains only tensile stresses, it is possible to construct it using a fabric or a cable net carrying the cladding. Fabric and cable net structures are usually prestressed to limit deflection under loading and control the internal stress distribution.

There are several examples of cladding systems for gridshells and cable nets, for example, membranes including fabric (Multihalle Mannheim; Millennium Dome in London), acrylic panels (Olympiastadion in Munich), glass (Diplomatic Club Heart Tent in Riyadh; the façade of the Kempinsky hotel in Munich), and timber panels (London Olympic Velodrome; Savill Building in Surrey; Volvohallen in Gothenburg).

Shell structures may be classified depending on their curvature. Most are doubly curved, meaning the surface curves in all directions or, more formally, the Gaussian curvature is non-zero everywhere, a concept discussed in more detail in section 3.2. A mathematical surface such as a dome, hyperbolic paraboloid, or hyperboloid may define the shell geometry. Shells may also be based on developable surfaces and can then be flattened onto a plane without distortion, for example, cylinders including 'generalised' cylinders and cones including conical surfaces.

However, boundary conditions are often such that no simple mathematical expression describes the complete geometry. Then form-finding techniques come into play, which, in early-stage design, usually solves the membrane equilibrium producing efficient bending-free surfaces. Of course, 'free-form surfaces' can also be used for shells but often with reduced efficiency. A recent example of the latter is the Google Mountain View complex. It was initially designed as a vast lightweight, transparent cable net roof covering the campus (S. Johnson 2015) but ended up as an array of heavy hanging opaque steel gridshells (Galiano 2020, pp. 30–35).

3.2   Geometry of surfaces

Due to the curved geometry of shells, considerable difficulties are encountered in finding basic equations describing their response to loading. Differential geometry provide necessary expressions to describe the shell geometry, and tensor notation is indispensable when, later, considering both geometry and structural concepts such as stress. The used notation follows closely that of Green and Zerna (1968). Kil'chevskiĭ (1965) and Domokos (1990) provide alternative notations for the same theory.

3.2.1   Position vector, base vectors, and the first and second fundamental form

Assuming the considered surface to be smooth and using a system of curvilinear coordinates denoted θ^1 and θ^2 defined on the surface, then the position vector

$$\mathbf{r}(\theta^1, \theta^2) = x(\theta^1, \theta^2)\mathbf{i} + y(\theta^1, \theta^2)\mathbf{j} + z(\theta^1, \theta^2)\mathbf{k}, \tag{3.1}$$

describes the relation between a point on the surface and its Cartesian coordinates x, y, z. $\mathbf{i}$, $\mathbf{j}$, $\mathbf{k}$ are orthogonal unit base vectors in the direction of Cartesian coordinate axes x, y, z, respectively. By convention, Greek indices range over the values 1, 2, so θ^α refers to both the θ^1 and the θ^2 coordinate, replacing the perhaps more commonly used notation u and v.

The *covariant base vectors* are given by

$$\mathbf{a}_\alpha = \mathbf{r},_\alpha = \frac{\partial \mathbf{r}}{\partial \theta^\alpha}, \tag{3.2}$$

which are such that $\mathbf{a}_1$ and $\mathbf{a}_2$ are tangential to curves $\theta^2 = $ constant and $\theta^1 = $ constant, respectively, see fig. 3.2a, and the comma denotes partial differentiation. In general, $\mathbf{a}_\alpha$ are neither unit vectors nor perpendicular to each other. There are also *contravariant base vectors* $\mathbf{a}^\alpha$ such that $\mathbf{a}^1$ and $\mathbf{a}^2$ are normal to surfaces $\theta^1 = $ constant and $\theta^2 = $ constant, respectively, see fig. 3.2b.

The covariant components of the metric tensor, also known as the *first fundamental form*, allows the computation of distances on the surface, and are given by

$$a_{\alpha\beta} = a_{\beta\alpha} = \mathbf{a}_\alpha \cdot \mathbf{a}_\beta. \tag{3.3}$$

The notation differs from Eisenhart (1947), who uses $g_{\alpha\beta}$, and from Struik (1961) and Rogers and Schief (2002), who uses E, F, and G.

The unit surface normal is given by

$$\mathbf{n} = \frac{\mathbf{a}_1 \times \mathbf{a}_2}{|\mathbf{a}_1 \times \mathbf{a}_2|} = \frac{\mathbf{a}_1 \times \mathbf{a}_2}{\sqrt{a}}, \tag{3.4}$$

$$a = |a_{\alpha\beta}| = |\mathbf{a}_1 \times \mathbf{a}_2|^2 = a_{11}a_{22} - (a_{12})^2. \tag{3.5}$$

Here the notation differs from Green and Zerna (1968) who uses $\mathbf{a}_3$ instead of $\mathbf{n}$. Its variation on the surface is described by the components of the normal curvature tensor,
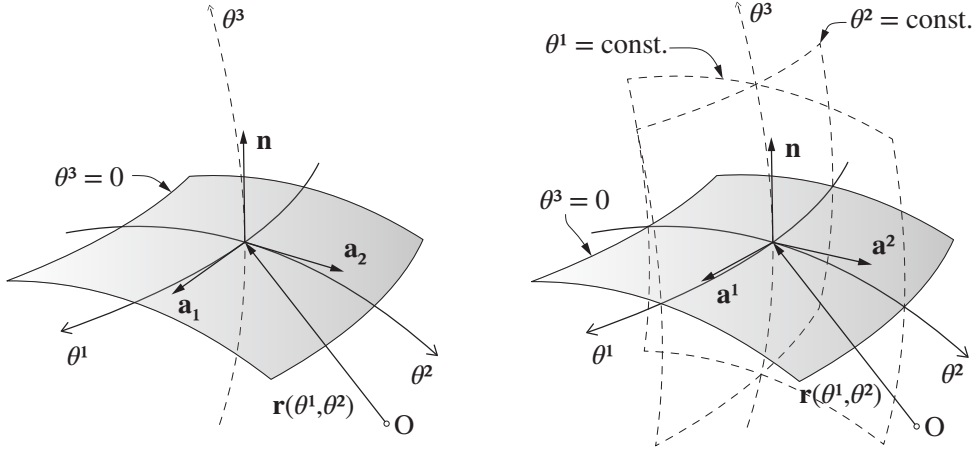
(a) *Covariant base vectors $\mathbf{a}_\alpha$ spans the surface tangent plane. Vector $\mathbf{a}_1$ is tangential to the curve $\theta^2 = constant$ and vice versa.*

(b) *Contravariant base vectors $\mathbf{a}^\alpha$. Vector $\mathbf{a}^1$ is normal to the surface $\theta^1 = constant$ and vice versa.*

Figure 3.2: *Surface with general curvilinear coordinates θ^1, θ^2 representing the middle surface of a shell ($\theta^3 = 0$). The position vector $\mathbf{r}(\theta^1, \theta^2)$ describes all points on the surface and $\mathbf{n} = \mathbf{n}(\theta^1, \theta^2)$ is the unit surface normal.*

or coefficients of the *second fundamental form*, given by

$$b_{\alpha\beta} = b_{\beta\alpha} = \mathbf{a}_{\alpha,\beta} \cdot \mathbf{n}. \tag{3.6}$$

Eisenhart (1947) uses $d_{\alpha\beta}$ and Struik (1961) and Rogers and Schief (2002) uses e, f, and g.

Occasionally, $\epsilon_{\alpha\beta}$ and $\epsilon^{\alpha\beta}$ are needed defined by

$$\left. \begin{array}{cc} \epsilon_{12} = -\epsilon_{12} = \sqrt{a}, & \epsilon^{12} = -\epsilon^{12} = 1/\sqrt{a} \\ \epsilon_{11} = \epsilon_{22} = \epsilon^{11} = \epsilon^{22} = 0 \end{array} \right\}. \tag{3.7}$$

3.2.2 Curvature and principal curvature directions

$a_{\alpha\beta}$ and $b_{\alpha\beta}$ are called *surface tensors* and are tensors under a surface transformation of coordinates (Green and Zerna 1968, p. 32) specific to the chosen coordinate system. Together they contain all the information about the *normal curvature* κ_n and twist of the surface, including the *principal curvatures*, denoted κ_I and κ_{II}, and their directions, the so-called *principal curvature directions* or, simply, *principal directions*. The principal curvatures are the maximum and minimum values of the normal curvature of the surface at each point. If $\kappa_I = \kappa_{II} = 0$ (a flat point) or $\kappa_n = $ constant (an umbilical point), then any direction is a principal directions, or else the surface has two principal directions. In the latter case, the principal directions are orthogonal and conjugate.

The invariant

$$K = \kappa_I \kappa_{II} = \frac{|b_{\alpha\beta}|}{a} = \frac{b_{11}b_{22} - (b_{12})^2}{a}, \tag{3.8}$$

is the *Gaussian curvature* of the surface, which can be used to define families of surfaces (see fig. 3.3), and

$$H = \frac{\kappa_{\mathrm{I}} + \kappa_{\mathrm{II}}}{2} = \frac{b_\alpha^\alpha}{2} = \frac{a^{\alpha\beta} b_{\alpha\beta}}{2}, \tag{3.9}$$

the *mean curvature* of the surface. To determine $a^{\alpha\beta}$ requires the contravariant base vectors $\mathbf{a}^\alpha$. For further details, see Adiels et al. (2018) containing a summary of the more important geometrical concepts presented in Green and Zerna (1968).

3.2.3 Asymptotic directions

Besides principal curvature directions on the surface, *asymptotic directions* are also of interest. These are directions on a surface with zero normal curvature. The angle φ between the principal and asymptotic directions on a surface can be determined using Mohr's circle of curvature (Nutbourne 1986). With the normal curvature on the horizontal axis, it is the circle through the points representing the principal curvatures, and so its radius is given by

$$R = \frac{\kappa_{\mathrm{I}} - \kappa_{\mathrm{II}}}{2} = \sqrt{H^2 - K}. \tag{3.10}$$

The angle between the horizontal axis and a line through the centre of the circle and the intersection of the circle and the vertical axis is equal to 2φ. The vertical axis represents the geodesic torsion τ_{g}, and so the principal directions have zero geodesic torsion. Figure 3.4 illustrates Mohr's circle of curvature for the same families of surfaces as shown in fig. 3.3, and for a minimal surface with negative Gaussian curvature (not a plane), the angle between the principal and asymptotic directions is always 45°.

3.2.4 Maps and coordinate alignment

So far, the discussion has concerned surfaces in real three-dimensional space that maps to the physical structure by translation, rotation, and uniform scaling. However, other mappings may be applied, offering alternative views of the geometry. These include the Gauss map and its stereographic projection. Both are conformal, meaning they preserve angles between lines. So is the Weierstrass-Enneper parametrization, which maps a complex number $\zeta = \theta^1 + i\theta^2$ to a real point $\mathbf{r}(\theta^1, \theta^2)$ on a minimal surface, albeit without any control of the direction of the coordinate system on the minimal surface.

Although not necessary, it is often convenient to align the coordinate system with something that makes sense physically, such as the cables in a cable net, the laths of a gridshell, the panelling of the formwork of a concrete shell, or the seams of a fabric. Such alignments may be obtained considering the equilibrium of the membrane shell.

3.3 Membrane theory of shells

In shell theory, the complicated three-dimensional equations for a continuum are reduced to two-dimensional form so that equations for stress resultants and stress couples are obtained instead of actual stress. The stress resultants, stress couples, and loads are

Paraboloid   Hyperboloid of two sheet

(a) *Elliptic surfaces $K > 0$*

Cylinder   Cone

(b) *Parabolic $K = 0$*

Hyperbolic Paraboloid   Hyperboloid of one sheet

(c) *Hyperbolic $K < 0$*

Schwarz D   Schwarz G   Schwarz P   Schreks surface

(d) *Minimal $K < 0$ and $\kappa_{\mathrm{I}} = -\kappa_{\mathrm{II}}$*
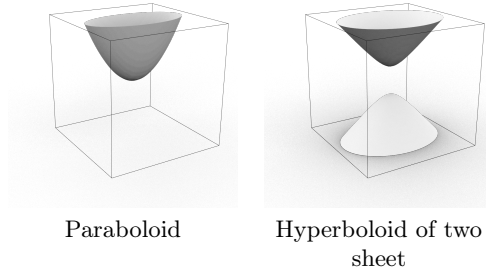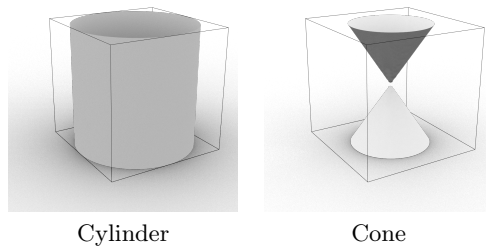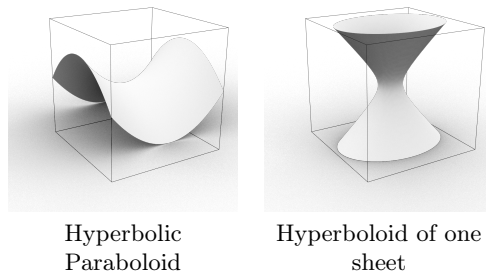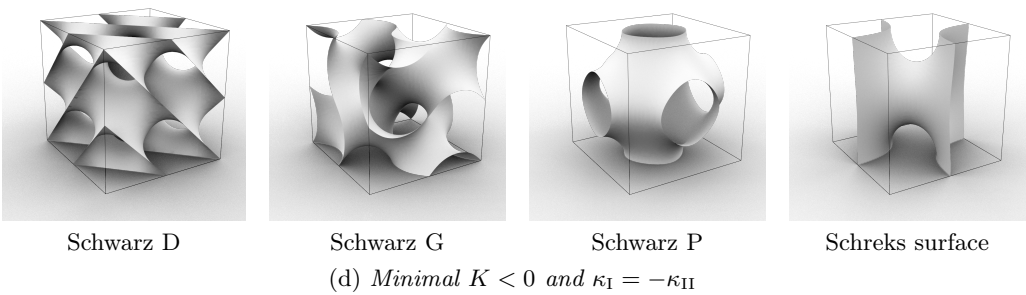
Figure 3.3: *Gaussian curvature for families of surfaces*

(a) *Elliptic*

(b) *Parabolic*

(c) *Hyperbolic*
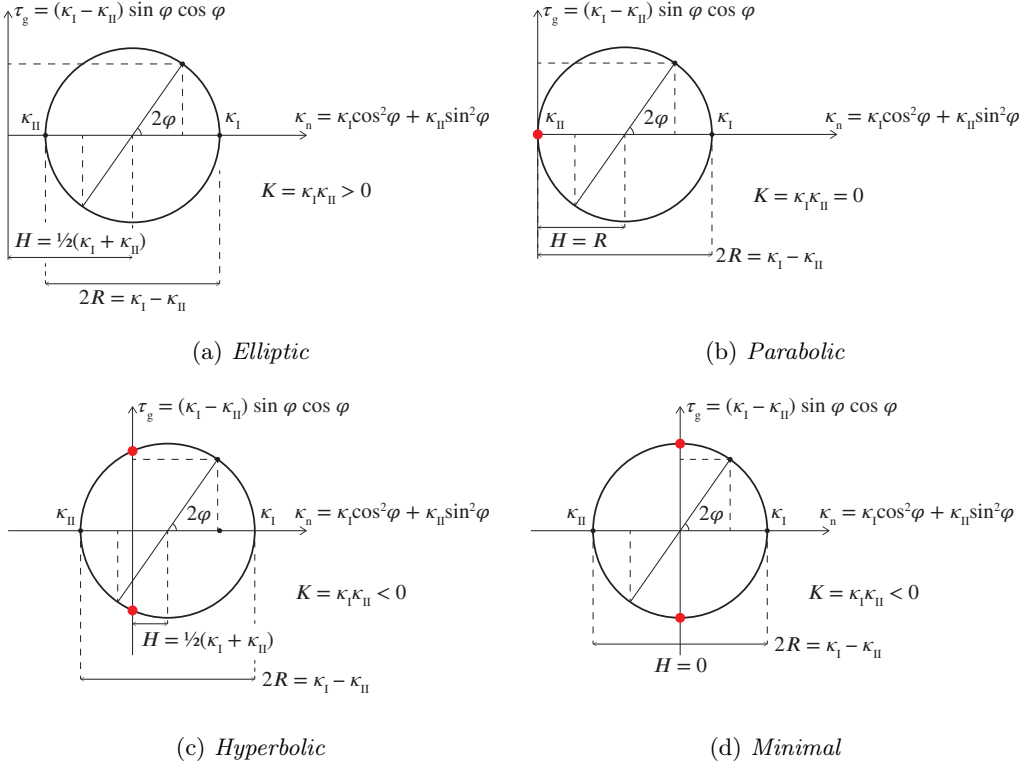
(d) *Minimal*

Figure 3.4: *Mohr's circle of curvature. Elliptic surfaces have no asymptotic directions, parabolic surfaces have exactly one, and hyperbolic surfaces two. Minimal surfaces with curvature are a type of hyperbolic surfaces where the angle between the principal and asymptotic directions always is 45°. A planar surface (not shown) has an infinite number of asymptotic directions, and any direction is an asymptotic direction.*

assumed to act on a surface position in the middle of the shell thickness, known as the shell middle surface, defined by the position vector $\mathbf{r}$. Neglecting bending action further simplifies the equations, and the theory is then known as the membrane theory of shells or the theory of membrane shells (Green and Zerna 1968, § 11).

This section provides a brief introduction to membrane theory of shells expressed in terms of stress resultant components denoted n with appropriate suffixes. The stress resultant components have measure force per cross-section width, and to obtain stress components measured as force per cross-section area, usually denoted using σ and τ with appropriate suffixes, division of the stress resultants with the shell thickness, t, is needed, for example,

$$\sigma_x = \frac{n_x}{t}, \quad \tau_{xy} = \frac{n_{xy}}{t}, \quad \sigma_y = \frac{n_y}{t}. \tag{3.11}$$

Note that while Paper F applies this notation, Paper E does not; Paper E expresses stress

resultants using σ_x, σ_y, and τ_{xy} instead of n_x, n_y, and n_{xy}, respectively.

Section 3.3.1 expresses the equilibrium equations in terms of general curvilinear coordinates referred to the tangent plane of the middle surface, section 3.3.2 in regular curvilinear coordinates referred to a base plane, and section 3.3.3 in regular coordinates, making expressions in tensor notation reduce to 'engineering' notation used by, for example, Timoshenko and Woinowsky-Krieger (1959). Neither way of expressing the equilibrium is superior to the others. Which to choose is influenced by the problem at hand and personal preference.

Section 3.3.2 also introduces the Airy stress function, enabling the expression of the stress state using a single scalar invariant function rather than several stress resultants, leading to the formulation of Pucher's equation in section 3.3.3.

3.3.1 General curvilinear coordinates

The static equilibrium of a membrane shell is given by

$$\left.\begin{array}{l} n^{\alpha\beta}|_\alpha + p^\beta = 0 \\ n^{\alpha\beta}b_{\alpha\beta} + p = 0 \end{array}\right\}. \tag{3.12}$$

p is the component of the load acting normal to the surface and p^α the components acting in the direction of θ^α, all measure per unit surface area. The components of the contravariant surface tensor $n^{\alpha\beta} = n^{\beta\alpha}$ are called stress resultants (Green and Zerna 1968, §§ 10.2, 11.1). The vertical bar means covariant differentiation (Green and Zerna 1968, § 1.12) with respect to the middle surface, so $n^{\alpha\beta}|_\alpha = n^{\alpha\beta},_\alpha + \Gamma^\beta_{\alpha\rho}n^{\alpha\rho} + \Gamma^\alpha_{\alpha\rho}n^{\rho\beta}$ where $\Gamma^\beta_{\alpha\rho}$ are the Christoffel symbols of the second kind. The physical stress resultants (per unit length) are given by

$$n_{(\alpha\beta)} = n^{\alpha\beta}\sqrt{\frac{a_{\beta\beta}}{a^{\alpha\alpha}}}, \tag{3.13}$$

but $n_{(\alpha\beta)}$ is not a tensor.

3.3.2 Plane curvilinear coordinates

The formulae of section 3.3.1 are related to the middle surface of the shell, but it is sometimes more convenient to refer the equations to a base plane so that the stresses are studied as seen when projected to the plane. Then the static equilibrium is given by

$$\left.\begin{array}{l} \bar{n}^{\alpha\beta}|_\alpha + \bar{p}^\beta = 0 \\ z|_{\alpha\beta}\bar{n}^{\alpha\beta} + \bar{p} - \bar{p}^\alpha z|_\alpha = 0 \end{array}\right\}, \tag{3.14}$$

where the covariant differentiation refers to the plane. The considered stress resultants and load components are those projected onto the plane, which the horizontal bar highlights. Here the notation differs from Green and Zerna (1968, § 11.2), who uses $k^{\alpha\beta}$, s, and s^β instead of $\bar{n}^{\alpha\beta}$, $\bar{p}$, and $\bar{p}^\beta$, respectively.

The first expression in eq. (3.14) is equivalent to the equilibrium of a plate when moment stresses are zero, and may alternatively be expressed in terms of ϕ, an invariant stress function of θ^1, θ^2 known as the Airy stress function (Airy 1863). Defining

$$\left. \begin{array}{l} \bar{n}^{\alpha\beta} = \epsilon^{\alpha\gamma}\epsilon^{\beta\rho}\phi|_{\gamma\rho} - A^{\alpha\beta} \\ \phi|_{\alpha\beta} = \epsilon_{\alpha\gamma}\epsilon_{\beta\rho}\left(\bar{n}^{\gamma\rho} + A^{\gamma\rho}\right) \end{array} \right\} , \tag{3.15}$$

where $A^{\alpha\beta}$ is symmetric and a particular integral of the equation

$$A^{\alpha\beta}|_\alpha = \bar{p}^\beta. \tag{3.16}$$

Then the evaluation of stresses in the membrane theory of shells is reduced to the solution of the linear differential equation for ϕ given by

$$\epsilon^{\alpha\gamma}\epsilon^{\beta\rho}z|_{\alpha\beta}\phi|_{\gamma\rho} = q, \tag{3.17}$$

where

$$q = z|_{\alpha\beta}A^{\alpha\beta} - \bar{p} + \bar{p}^\alpha z|_\alpha, \tag{3.18}$$

and q contain all the load acting on the shell.

It follows that ϕ has the units of force times length, which is the same as bending moment, and the gradient of ϕ has the units of force.

3.3.3 Plane regular coordinates

Choosing a regular Cartesian coordinate system in the plane, the base vectors of the coordinate system are orthogonal constant unit vectors. Then, from eq. (3.5), $a = 1$, and the Christoffel symbols $\Gamma^\beta_{\alpha\rho}$ vanish when performing covariant differentiation. Therefore, eq. (3.17) simplifies to

$$z_{,11}\phi_{,22} - 2z_{,12}\phi_{,12} + z_{,22}\phi_{,11} = q. \tag{3.19}$$

If $\theta^1 = x$ and $\theta^2 = y$ and writing the partial derivatives explicitly, then the equation become

$$\frac{\partial^2 z}{\partial x^2}\frac{\partial^2 \phi}{\partial y^2} - 2\frac{\partial^2 z}{\partial x\partial y}\frac{\partial^2 \phi}{\partial x\partial y} + \frac{\partial^2 z}{\partial y^2}\frac{\partial^2 \phi}{\partial x^2} = q, \tag{3.20}$$

which is equivalent to eq. (f), article 113 in Timoshenko and Woinowsky-Krieger (1959), who attribute the first use of a stress function in this way to Pucher (1938). Furthermore, considering only vertical loading, following from equation eq. (3.18)

$$q = -\bar{p}, \tag{3.21}$$

and from eqs. (3.7) and (3.15)

$$\bar{n}^{\alpha\beta} = \epsilon^{\alpha\gamma}\epsilon^{\beta\rho}\phi_{,\alpha\beta}. \tag{3.22}$$

Finally, with $a = 1$, from eq. (3.13) follows that the stress resultants and the physical stress resultants are the same, and the above expression expands to

$$\left. \begin{array}{l} n_x = \bar{n}_{(11)} = \bar{n}^{11} = \phi_{,22} \\ n_{xy} = \bar{n}_{(12)} = \bar{n}^{12} = -\phi_{,12} \\ n_y = \bar{n}_{(22)} = \bar{n}^{22} = \phi_{,11} \end{array} \right\} . \tag{3.23}$$

3.4 Airy stress function

The Airy stress function ϕ is an invariant function of two coordinates on a reference plane and describes the stress state in an associated continuous membrane-action structure, see fig. 3.5. Solving for ϕ in Pucher's eq. (3.20) is referred to as stress finding, whereas treating ϕ as the known and solving for the geometry z as form finding. The discreet version of ϕ, with planar patches joined via folds and cuts representing concentrated forces and moments respectively, can model the equilibrium in planar pin-jointed bar structures, see fig. 3.6, providing a link to graphic statics.

(a) *Uniform tension* (b) *Non-uniform tension* (c) *Mono-axial tension*
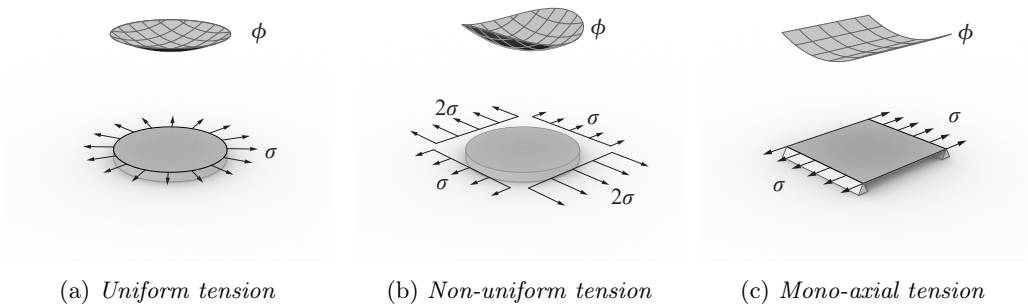
Figure 3.5: *Airy stress function for skin on drum (a and b) and skin stretched between parallel supports (c)*

(a) *Differently compressed bars and tensioned ties* (b) *Hinged frame and tensioned tie.* (c) *Stiff frame and differently tensioned ties*

Figure 3.6: *Airy stress function for exterior bars and frames with interior diagonal ties*

3.4.1 Stress finding

Pucher's eq. (3.20) is a differential equation that solves the unknown internal stress state ϕ given the shape of the membrane shell, z, and the applied loading, q. The equation is

elliptic if the Gaussian curvature of z is positive ($K > 0$), hyperbolic if negative ($K < 0$), and parabolic if zero ($K = 0$). In general, it is not possible to say whether or not there exists a solution that satisfies the boundary conditions, particularly at a free edge where the stresses are zero. If it is not possible to find a solution, then the structure cannot stand by membrane action alone and some bending will be required. However, it is possible to show that a hyperboloid of revolution attached to the ground, such as a cooling tower, can work by membrane action, as can any closed convex surface (Cohn-Vossen 1927).

3.4.2 Form finding

The considerations of section 3.4.1 apply in the same way if z is the unknown instead of ϕ in eq. (3.20), and solving z is the essence of the form-finding of membrane-action shells. For example, if the structure is all in tension or all in compression, then ϕ is a bowl-shaped surface, and the differential equation is elliptic, and a paraboloid of revolution have constant curvature in the radial direction and therefore represent a uniform stress state (fig. 3.5a). If there is both tension and compression, the equation can be a mixture of elliptic, hyperbolic, and parabolic, making it much more challenging to solve.

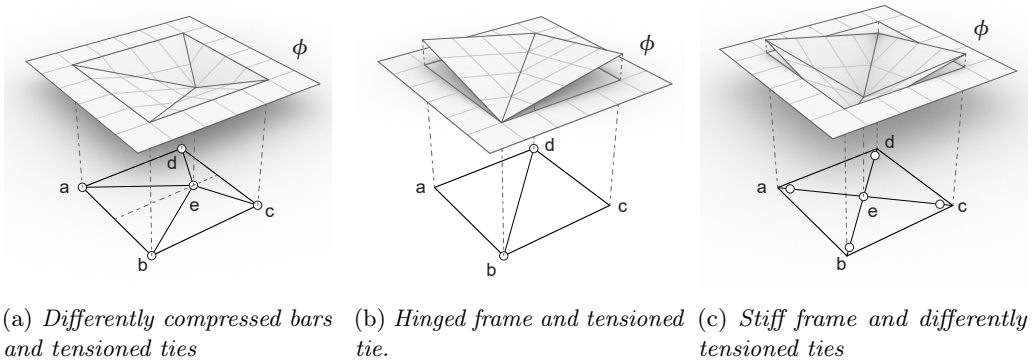When the membrane equilibrium equations are too complex to solve analytically, which is generally the case, physical or numerical models come into play. During the form-finding process, the geometry is adjusted from an initial state to the form-found state, and so the model has to be a mechanism. As the built structure cannot be a mechanism, the form-found one must be 'frozen' when constructed either by adding bending stiffness or bracing.

Physical models might involve hanging chains which will be inverted to form a compression structure (Graefe 2020) as explained by Hooke (1675), a technique pioneered by Antoni Gaudí (Huerta 2006) and refined by Frei Otto (Burkhardt et al. 1978; Happold and Liddell 1975), see fig. 3.7. Heinz Isler (1926–2009) used damp hanging fabric, which he froze and inverted to form-find his compressive concrete shells (Chilton 2020), and Almegaard (2014) discusses the relation between Isler's method and the Airy stress function. The model may also involve a combination of soap film, which approximates a minimal surface, and cotton threads in tension and masts in compression, also used by Otto and Rasch (1995).

Most numerical form-finding methods simulate a physical model. Veenendaal and Block (2012) provides an overview and comparison of structural form-finding methods for general networks, and a condensed version is included in the book *Shell structures for architecture: form finding and optimization* (Adriaenssens et al. 2014) which provides a comprehensive introduction to the topic. Two of the more commonly used methods are the *force density method* and the *dynamic relaxation method*. In the force density method (Linkwitz and Schek 1971; Schek 1974), *force densities*, also known as *tension coefficients* (Southwell 1920), specifies the desired ratio between member force and length, and a single system of linear equations is solved. In the dynamic relaxation method (Day 1965; Barnes 1977), the equilibrium equations are solved explicitly by iteration. Implicit methods, such as the *Newton–Raphson method*, may also be used for form-finding. The *thrust network analysis* (Block and Ochsendorf 2007; Block 2009; Block and Lachauer 2014) adopts a graphical approach and targets the design of compression shells such as
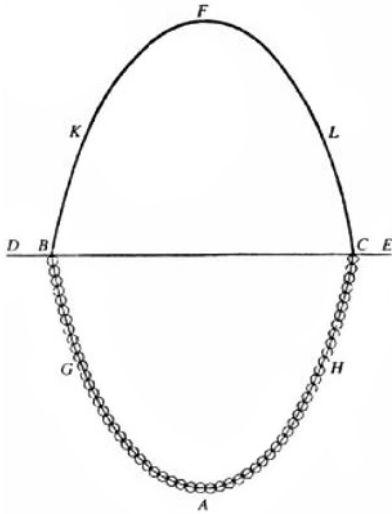
(a) *Poleni's drawing of Hooke's analogy between an arch and a hanging chain*

From plate D in G. Poelini (1748) Memorie istoriche della gran cupola del Tempio Vaticano

(b) *Standing tension arch loaded with balloons*
Courtesy of Sanne Sehlström

(c) *A 'Frei Otto eye' form-found using soap film and cotton threads*
Courtesy of Emil Adiels
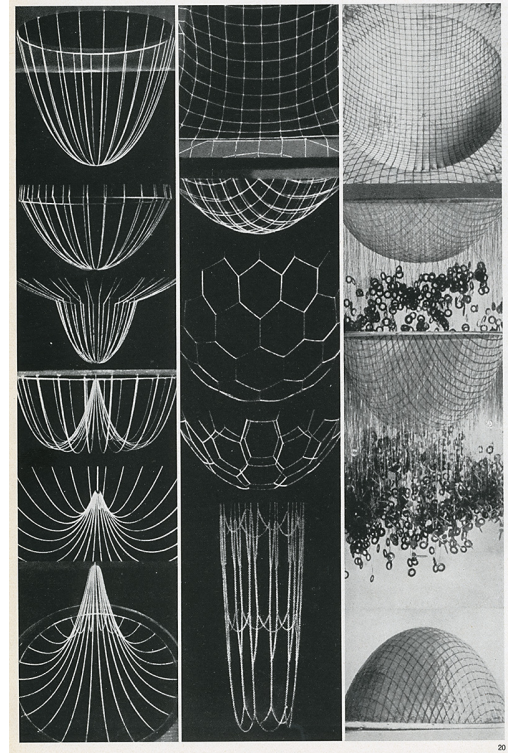
(d) *Chain models by Frei Otto*
Published in Casabella 301 1966, p. 40

Figure 3.7: *Form-finding techniques*

dry stone masonry (Rippmann, Van Mele, et al. 2016).

Based on a geometrical finite elements, Arcaro, Klinka, and Gasparini (2013) form-finds minimal surfaces formulating the problem as an equality constrained minimisation problem. Miki et al. (2020) solves the geometry given the desired stress state defined by a piece-wise smooth hyperbolic Airy stress function using isogeometric NURBS elements, allowing the form-finding of shells containing both compression and tension.

3.4.3 Graphic statics

Regardless of whether using the Airy stress function to study planar or shell structures, eq. (3.23) tells that the stress in the direction of one coordinate axis, say the x-axis, is the rate of change of slope of ϕ in the perpendicular direction, so $n_x = \phi_{,22} = \phi_{,yy}$, leading to quantities such as $\phi_{,xx}$ and $\phi_{,xy}$ discussed as the 'curvature' or 'twist' of the ϕ-surface. If there is no curvature in one direction, then there is no stress in the perpendicular direction, and a planar region in ϕ represents a stress-free area in z (fig. 3.5c). Similarly, if ϕ has twice the curvature in one direction than in the perpendicular, there is twice the stress in the corresponding direction than in the perpendicular (fig. 3.5b). Computer graphics makes the visualisation of the shape of ϕ and its curvature easy, and the same applies to z, altogether offering a tangible way to understand their interplay, similarly as in graphic statics.

Graphic statics establishes a reciprocal relation between the form and force diagram (fig. 3.8). It originates from the 18th and 19th centuries through the work of Varignon (1725), Culmann (1866), Cremona (1872), Maxwell (1864a), Maxwell (1870), and Rankine (1858), its chronology is laid out by Kurrer (2008), and Allen and Zalewski (2009) is often used to introduce the method. Computer implementations make the drawing of the diagrams faster (Greenwold and Allen 2003; Van Mele, Brunier-Ernst, and Block 2009; Rippmann, Lachauer, and Block 2012). Van Mele and Block (2014) presents a general algebraic implementation which, given a form diagram, allows the direct generation of a force diagram. Todisco et al. (2015) and Todisco (2016) applies graphic statics on post-tensioned funiculars and Beghini et al. (2014) combines graphic statics with structural optimisation. Alic and Åkesson (2017) extends algebraic statics to be bi-directional so that changes in the force diagram generate the form diagram, and provides an example of a prestressed funicular, much similar to Conzett's Wasserfallbrücke (Dechau 2013), where alterations of the prestressing force generate changes in the form diagrams.

Nielsen (1964) showed how to design space frame structures using the Airy stress function as a numerical 'moment field method.' Perhaps because Nielsen wrote in Danish, his work is little known. But he effectively extended extended graphic statics to three dimensions, a topic which has received much attention during the last couple of decades (Block and Ochsendorf 2007; Akbarzadeh, Van Mele, and Block 2013; Akbarzadeh, Van Mele, and Block 2015) and applied to the design of structural masonry (Fraternali 2010; Rippmann, Van Mele, et al. 2016) and post-tensioned funiculars (Perez-Sala et al. 2018).

The three-dimensional applications draws upon the fact that an Airy stress function discretized into a polyhedral represents the force equilibrium of a planar bar framework. After resolving the horizontal forces in the planar network, it is 'lifted' into space to complete also the vertical equilibrium. Such structures are sometimes called '2.5D-
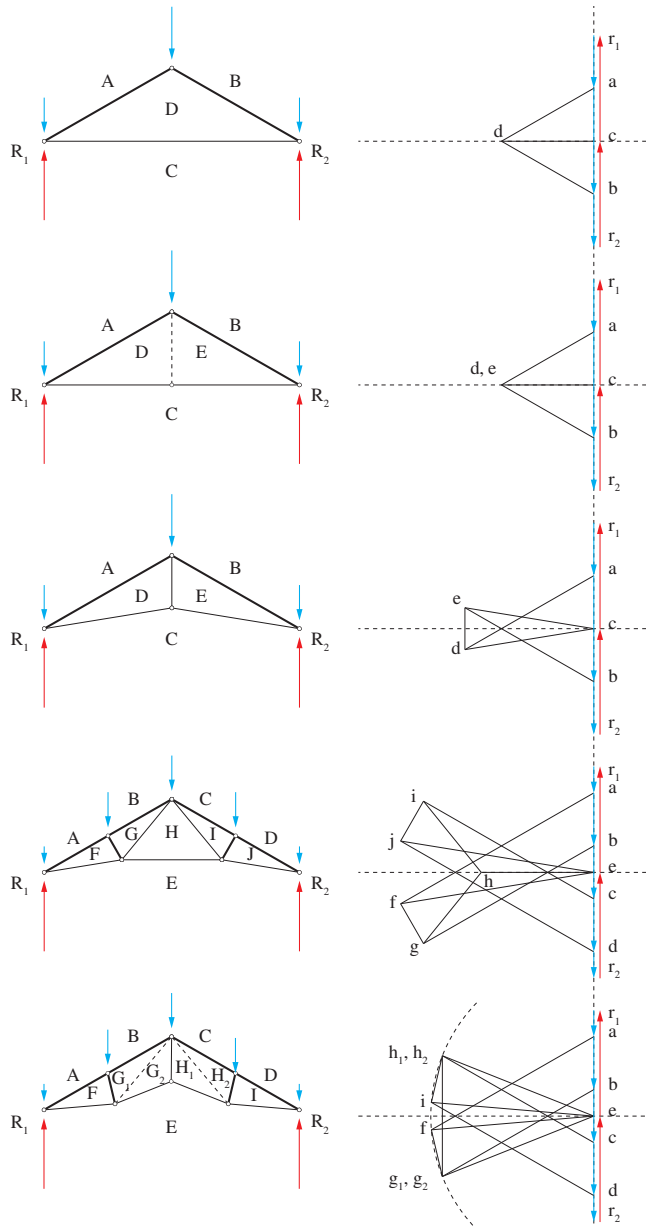
Figure 3.8: *Graphic statics using Bow's notation applied on equal span and rise roof trusses resisting the same load. The force in a member in the form diagram (left) between, say, fields* A, D *in the first three trusses is given by the length of the parallel line between points* a, d *in the corresponding force diagram (right). In the form diagram, compressed bars are drawn thick, tensioned bars thin, and those that carry no load dashed; in case of uneven loading on the last truss, dashed bars must be included, else activating a mechanism.*

44

structures.' In the Airy polyhedral, all curvature concentrate into 'folds' in between planar faces, and the planar projection of the polyhedral is the form diagram of the framework, establishing a direct relation to graphic statics. Furthermore, the slopes of the polyhedral faces map to the vertices of the force diagram laying in the xy-plane such that a face with (non-unit) normal $\mathbf{N} = (-\phi_{,x}, -\phi_{,y}, 1)$ maps to the vertex with coordinates given by

$$\mathbf{k} \times (\mathbf{N} - (\mathbf{N} \cdot \mathbf{k})\,\mathbf{k}) = (-\phi_{,y}, \phi_{,x}, 0)\,, \tag{3.24}$$

where $\mathbf{k}$ is the unit base vector in the direction of the z-axis.

Recently, Williams and McRobie (2016) introduced discontinuous Airy stress functions for planar structures providing means to interpret 'cuts' in the stress function as in-plane moments about the vertical axis and associated shear forces.

Drawing upon the idea of the folds, graphic statics and polyhedral Airy stress functions have been explored during this research, resulting in a computational tool called *Fold Your Forces*. The tool enables interactive folding of the stress function with automatic computation of the forces in the folds and the corresponding force diagram. Figure 3.9 illustrates an example of its application.

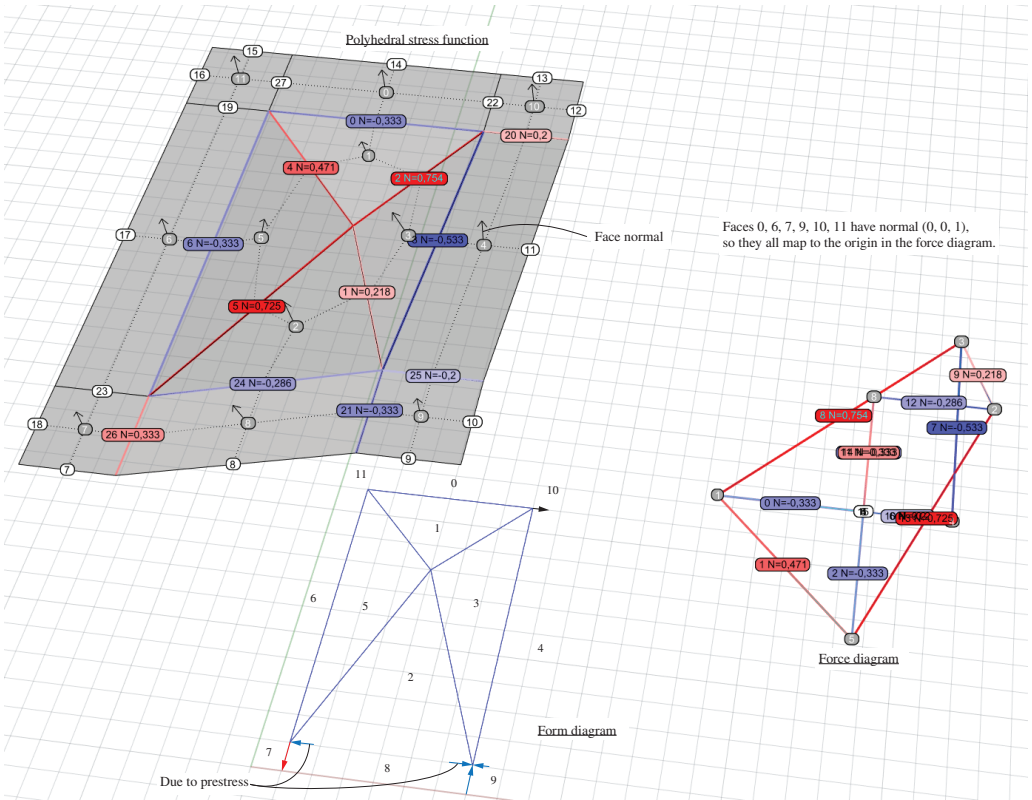Figure 3.9: *A prestressed pin-jointed wind brace withstanding an applied load at the top right corner analysed using* Fold Your Forces. *The projection of the polyhedral stress function onto the plane gives the form diagram and the normal of the polyhedral stress faces map to the vertices in the force diagram. Bars are coloured according to the magnitude of the force they contain where red is tension and blue compression.*

4 Methodology

Figure 4.1 conceptually visualise the methodology applied to meet the objectives presented in section 1.6.
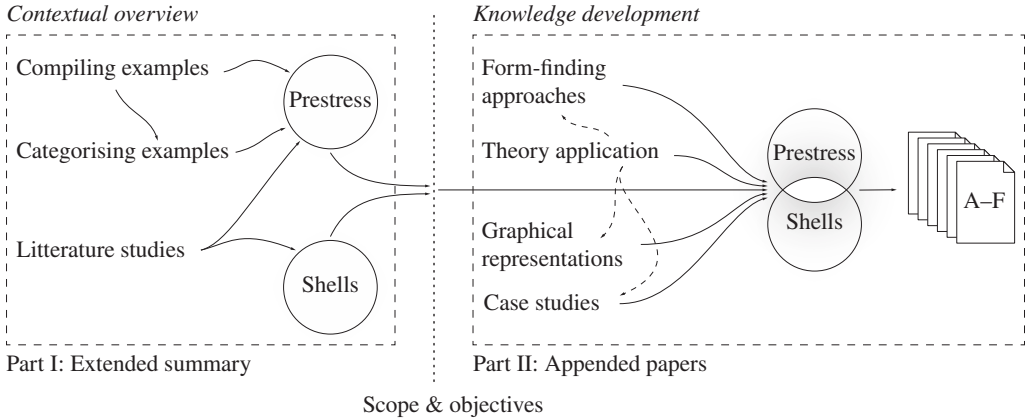
Figure 4.1: *Thesis methodology*

4.1 Contextual overview

The contextual overview, summarised in chapters 2 and 3, aims to answer the general questions proposed in section 1.4 and helps introduce and establish the fields of prestressing and shell structures on their own.

Chapter 2 concerns prestressing, drawing upon literature studies and a collection of prestressed objects. The chapter outlines the conditions for prestressing and its influence on structural behaviour. It concludes with a distinction between active and inactive prestress. Furthermore, it proposes general objectives and strategies for prestressing derived by applying various categorisations of the objects in the compiled collection.

Chapter 3 discusses shell structures based on literature studies, providing an overview of different shell structures, a brief introduction to classical differential geometry, and membrane shell theory, leading to Pucher's equation. The chapter includes an overview of stress-finding and form-finding approaches. Moreover, it presents graphical and numerical representations of the Airy stress function and its relation to graphic statics, an area of recent research interest, making the interplay between form and force tangible, helping to inform design decisions.

4.2 Knowledge development

Section 1.5 introduces a scope focusing the research on the application of prestressing on shell structures, and section 1.6 lists the research objectives. The following describes

the general methodology applied to meet the objectives. The appended papers contain further details on the methodology relevant for the respective study.

Theory application:

Literature studies followed by the combination and application of several theories provides means to understand the conditions for the prestressing of shells and what influence the prestressing has on the structural behaviour. Considered theories are, for example, classical differential geometry, the rigidity of pin-jointed bar networks, and elasticity. These studies have a direct influence on all other activities undertaken during this research.

Form-finding approaches:

Studies on equilibrium for specific types of prestressed membrane-action shells facilitate analytical and numerical form-finding approach development, where the numerical primarily draw upon the dynamic relaxation method.

Graphical representations:

Graphic statics and recent extensions are scrutinised and inform the development of representations suitable for prestressed shells, making the interplay between form and forces tangible, supporting the design of material efficient prestressed shell structures.

Case studies:

The influence of prestressing and how to choose the prestress level is explored by studying existing prestressed shell structures applying shell theory and differential geometry and, in the case of cylindrical shells, comparing results with those obtained using Euler-Bernoulli beam theory.

5 Summary of appended papers

5.1 Paper A

Prestressed gridshell structures

Most form-finding methods for grid-shells produce a grid of tensioned members, and by flipping the geometry upside down, the members become compressed. However, auto-equilibrated prestressed gridshell must contain both compression and tension members. Paper A extends dynamic relaxation by introducing virtual negative masses, effectively moving unstable geometrical configurations towards stable configurations. The method enables the form-finding of shells containing a combination of compression and tension members, which may lie in one or several layers. The desired stress state in each member is specified using force densities representing a state of prestress and possibly the stresses arising due to external loading. The method allows member length constraints met by updating the force densities during the form-finding.

5.2 Paper B

Unloaded prestressed shell formed from a closed surface unattached to any supports

Not all surfaces can be actively prestressed, and Paper B begins to answer the question 'under what conditions can an unloaded shell formed of a closed surface unattached to any support contain a state of membrane stress which can be induced by prestressing?' A network of pin-jointed bars approximating a sphere cannot be prestressed since it forms a rigid structure without any mechanisms; only statically indeterminate models can be prestressed according to Maxwell's rules for bar frameworks (Maxwell 1864b; Calladine 1978). Both the Cohn-Vossen theorem (Cohn-Vossen 1927; Hsu 1960) and Cauchy's rigidity theorem (Cauchy 1813) confirms this conclusion. The Cohn-Vossen theorem state that any closed surface with everywhere positive Gaussian curvature is rigid and that, if unloaded, cannot contain membrane stresses. Cauchy's rigidity theorem state that a convex polyhedron is rigid. However, a torus has both negative and positive Gaussian curvature. If approximated by pin-jointed bars, it forms a mechanism under certain topological situations and can, therefore, by the logic of Maxwell's rule, be prestressed by shortening six different bars or any linear combination thereof.

5.3 Paper C

Tensioned principal curvature cable nets on minimal surfaces

A fine net of cables forming a pattern of curvilinear squares approximates a minimal surface, subjected only to the limitation of the fineness of the grid. Such nets may follow principal curvature directions or asymptomatic directions. Paper C describes both an analytical and a numerical approach for the form-finding of minimal surfaces with a

principal curvature net, and 45° rotation of the grid gives the asymptotic directions. Both approaches apply to any minimal surface whose boundaries are either principal curvature or asymptotic directions or a combination. Straight lines and cable boundaries form asymptotic lines (Williams 2011), and a minimal surface that is normal to a sphere has a principal curvature direction as its boundary.

5.4 Paper D

The analytic and numerical form-finding of minimal surfaces and their application as shell structures

Paper D complements Paper C by providing a quick and easy numerical algorithm that automatically produces a minimal surface and the principal curvature coordinates simultaneously. The algorithm applies to any minimal surface whose boundaries are either principal curvature or asymptotic directions, or a combination of the two. Benchmarks show that the algorithm executes up to 60 times faster computed in parallel threads on the graphics card (GPU) than serial computation on the central processing unit (CPU). In addition, a discontinuous Airy stress function illustrates the load-bearing behaviour of a surface materialised with members following asymptotic directions loaded over a small patch. The patch load gives rise to a force couple acting along with the asymptotic members that bound the patch. The same happens in continuous surfaces, and by taking the small patch to the limit, the resulting point load gives rise to a moment along with the asymptotic directions.

5.5 Paper E

Design of tension structures and shells using the Airy stress function

Discontinuities in the Airy stress function for in-plane stress analysis represent forces and moments in connected one-dimensional elements (Williams and McRobie 2016). Paper E extends this representation to curved membrane-action structures, such as shells and cable nets, and graphically visualise the internal stresses and section forces at the boundary necessary for equilibrium. Hyperbolic paraboloid structures are studied using the approach, serving as demonstrations of its application. Firstly, the membrane stresses and edge forces of two of Félix Candela's concrete shells are determined and visualised (Candela 1960). Secondly, the prestressing needed for three existing cable nets is determined, allowing the exploration of its influence on the edge-beam bending moment. The considered structures are the Scandinavium arena from 1971 by architect Poul Hultberg and engineer Gunnar Kärrholm (Kärrholm and A. Samuelsson 1972), the London Olympic Velodrome from 2011 by Hopkins Architects and Expedition Engineering (Arnold et al. 2011; Wise et al. 2012), and the Wolfsburg Autostadt Roof from 2013 by Graft Architects and Schlaich Bergermann Partner (M. Schlaich and Behnke 2014).

5.6 Paper F

Does Torroja's prestressed concrete Alloz aqueduct act as a beam or a shell?

The study of existing structures may provide new insights. Paper F presents a study on Eduardo Torroja's prestressed concrete Alloz aqueduct from 1939. The aqueduct is a graceful and elegant structure, and the paper examines its structural behavior to see whether it acts as a beam or a shell. This is of interest regarding the Alloz aqueduct itself and for the design of similar structures in the future. The paper applies two alternative approaches available at that time. Firstly, the membrane theory of shells, effectively assuming the aqueduct walls are infinitely flexible in bending, and secondly, the Euler-Bernoulli 'plane sections remain plane' elementary beam theory. It reviews Torroja's calculations based on an elaboration of the Euler-Bernoulli beam theory known as the Griffith-Taylor theory for the bending of cantilevers.

Both the membrane shell and Euler-Bernoulli beam theory require a prestress to be applied along the longitudinal edges of the channel. However, the level of prestress in the Alloz aqueduct is consistent with the beam theory, which seems the most appropriate approach. In general, increased prestressing may reduce the wall bending moments, allowing for reduced cross-section thickness, although with increased deformations.

Whether or not a structure of this type act as a shell depends upon the thickness of the wall. The thinner the wall, the more it acts as a shell. The wall thickness of the Alloz aqueduct is sufficient for it to act mainly as a beam.

6 Conclusions and future works

This dissertation aims to provide an increased understanding of prestressing and its application to shell, fabric, and cable net structures and improved means for their design. It seeks answers to three main research questions and, in doing so, contributes to the fields of architectural and structural design and structural optimisation and applies differential geometry.

The extended summary discusses the general phenomena and structural behaviour of prestressing and shells on their own, whereas the presented studies focus on their combination. Understanding phenomenons and behaviour are necessary for the early-stage conceptual design to guide design choices resulting in sound engineering and high-quality architecture. This thesis contributes with several tools and representations that may be used in a collaborative conceptual design situation, offering multiple ways to explore design possibilities.

6.1 Summary of contributions

6.1.1 Question 1

Question 1 is twofold.

The first part is: *Can any shell be prestressed?* The short answer is: no, not all shells can be prestressed. To better answer the question, the thesis proposes the concept of active and inactive prestress. Then the answer is: no, not all shells can be actively prestressed. The membrane stress must be statically indeterminate to actively prestress a shell, a condition influenced by the shell geometry and the boundary conditions. However, even if a shell is statically determinate and therefore cannot be actively prestressed, it may still be inactively prestressed, for example, by making small changes in the configuration, producing local areas which are statically indeterminate possible to prestress.

The second part is: *For those that can, what is the meaning and influence of prestressing?* This question is broad, and the general answer is: it depends. Prestressing is introduced to improve the performance of a structure, and as discussed in section 2.4, there are several objectives with prestressing in general. These objectives do also apply to prestressed shells.

The main contributions connected to question 1 are:

- An unloaded sphere unattached to any support cannot be actively prestressed by membrane stresses alone, but a torus can (Paper B).

- A concentrated prestress force in the longitudinal edges is a condition for the equilibrium of cylindrical membrane shells (Paper F).

- Prestressing minimises the wall bending moments of beams with cylindrical cross-sections enabling thinner cross-sections, and at the limit, the structural behaviour is that of a cylindrical membrane shell rather than of an Euler-Bernoulli beam (Paper F).

6.1.2 Question 2

The second question is: *How can prestressed shells be form-found using analytical and numerical approaches?* The thesis provide an overview of several form-finding approaches resulting in geometries which work predominately by membrane action. By modifying the methods, they can include a state of prestress. The presented papers contain some suggestions of such modifications, concentrating on shells that are minimal surfaces or gridshells.

Minimal surfaces

Surfaces with uniform surface tension are minimal. Materialised using a grid of cables following principal curvature directions, it is possible to produce 'true' tensioned minimal surfaces, limited only by the fineness of the grid.

The main contributions to the form-finding of prestressed minimal surfaces are:

- An analytical and a numerical approach for the form-finding of minimal surfaces with principal curvature coordinates.

- A minimal surface that is normal to a sphere has a principal curvature direction as its boundary.

The analytic approach uses a single function of a complex variable valid for every minimal surface with principal curvature coordinates (Paper C). The numerical approach automatically produces a minimal surface and the principal curvature coordinates at the same time and can be applied to any minimal surface whose boundaries are either principal curvature or asymptotic directions or a combination of the two (Paper C). An implementation using dynamic relaxation executed in multiple parallel threads on the GPU shows significant speed gain compared to serial execution on the CPU, offering near-instant results even for large systems (Paper D).

Gridshells

Most numerical form-finding methods for gridshells simulate a physical model which has to be stable to achieve equilibrium, and they result in a structure with members only in either tension or compression.

The main contributions to the form-finding of gridshells are:

- A numerical method for the form-finding of gridshells containing both tension and compression elements (Paper A).

6.1.3 Question 3

The third question is: *How can prestress in shells be represented and chosen, aspiring for efficient structural performance?* The question is explored using the Airy stress function. The stress function can be understood as a surface providing a graphical representation of the internal stress state of a shell, which may or may not be prestressed.

Representations

The use of proper representations can ease the often challenging understanding of the interplay between form and forces in shell structures. The main contributions are:

- The Williams and McRobie (2016) discontinuous Airy stress function is extended from flat structures to curved shells, allowing moments and shear forces in edge beams of shell structures to be quantified and thus designed (Paper E).

Stress finding

To find the stress state in a structure is central to understanding its behaviour, and such understanding is itself a key to apply prestressing correctly. The main contributions are:

- A method based on a discrete Airy stress function to explore the prestress level and section forces and moments in shell structures (Paper E).

- A patch load on a minimal surface result in a pair of concentrated compression and tension forces acting along with the asymptotic lines that bound the patch, which at the limit become a moment (Paper D). The same applies to any surface with negative Gaussian curvature.

The concentrated section forces and moments are, however, only indicating an idealised behaviour guiding design choices; in a continuous surface, strain compatibility will dissipate such forces and moments, spreading them over a larger area.

6.2 Future works

With additional literature studies and further examples, the proposed prestressing objectives and strategies may be developed into a publication on its own, either as a review article intended for the research community or a popular science publication targeting practitioners. Such work could also elaborate further on the concept of active and inactive prestress. Furthermore, present and discuss types of prestressed shells.

The form-finding process associates with the early design stages. The application and usefulness of the suggested form-finding approaches are yet to be studied, for example, in case studies of design projects. Such studies would provide valuable knowledge regarding their usefulness and possible improvements. Furthermore, case studies would enable the study of the interaction and collaboration between architects and engineers during their mutual effort of designing a prestressed shell, leading to sound engineering and high-quality architecture. To what extent do the suggested form-finding approaches and representations enhance the understanding of the underlying phenomenons?

The *Fold Your Forces* computer tool (see fig. 3.9) implements the concepts of folds in a polyhedral Airy stress function allowing interactive modelling of the stress function with direct response on forces in the associated pin-jointed planar bar framework. Future works should finalise the tool and enable means to model 'cuts' in the stress function, allowing additional interactive modelling of moments and shear forces in trusses. Furthermore, the ability to interactively model piece-wise smooth Airy stress functions should be

investigated, extending the functionality from discrete networks to continuous structures and possibly shells, similarly as in Paper E.

Paper B only begins exploring the conditions to prestress an unloaded shell formed from a closed surface unattached to any supports. It concludes that a torus can be prestressed in such a way and that there is certainly more to discover. Further studies may reveal these unknown surfaces and conditions or prove the hypothesis wrong.

References

Addis, B. (1994). *The Art of the Structural Engineer*. Ed. by A. Bridges. London: Artemis London Limited. ISBN: 1874-056-41-2.

— (2007). *Building: 3000 years of design engineering and construction*. London ; New York: Phaidon.

Adiels, E. et al. (2018). "The use of virtual work for the formfinding of fabric, shell and gridshell structures". *Proceedings of the Advances in Architectural Geometry conference 2018*. Ed. by L. Hesselgren et al. Klein Publishing, pp. 286–315. ISBN: 978-3-903015-13-5.

Adriaenssens, S. et al., eds. (Apr. 2014). *Shell structures for architecture: form finding and optimization*. London: Taylor & Francis - Routledge.

Airy, G. B. (Dec. 1863). IV. On the strains in the interior of beams. *Philosophical Transactions of the Royal Society of London* **153**, 49–79. DOI: `10.1098/rstl.1863.0004`.

Akbarzadeh, M., T. Van Mele, and P. Block (2013). "Equilibrium of spatial structures using 3-D reciprocal diagrams". *Proceedings of the International Association for Shell and Spatial Structures (IASS) Symposium 2013*.

— (June 2015). On the equilibrium of funicular polyhedral frames and convex polyhedral force diagrams. *Computer-Aided Design* **63**, 118–128. DOI: `10.1016/j.cad.2015.01.006`.

Aldinger, I. L. (Mar. 2016). Frei Otto: heritage and prospect. *International Journal of Space Structures* **31**.1, 3–8. DOI: `10.1177/0266351116649079`.

Alic, V. and D. Åkesson (Dec. 2017). Bi-directional algebraic graphic statics. *Computer-Aided Design* **93**, 26–37. DOI: `10.1016/j.cad.2017.08.003`.

Allen, E. and W. Zalewski (2009). *Form and forces: designing efficient, expressive structures*. John Wiley and Sons. ISBN: 978-0-470-17465-4.

Almegaard, H. (2014). Pucher, Isler and form finding of shells. *Abstract from Nordic Society for Structures in Architecture Meeting*.

Angelo and N. N. Maggi (2003). *John Soane and the Wooden Bridges of Switzerland; Architecture and the culture of technology from Palladio to the Grubenmanns*. Archivio del Moderno, Acacemia die architettura, Mendriso / Sir John Soane's Museum. ISBN: 88-87624-24-0.

Arcaro, V. F., K. K. Klinka, and D. A. Gasparini (2013). Finite elements for geometrical minimal shape. *Forma-Society for Science on Form* **28**.1, 7–16.

Arnold, R. et al. (Nov. 2011). Delivering London 2012: the Velodrome. *Proceedings of the Institution of Civil Engineers - Civil Engineering* **164**.6, 51–58. DOI: `10.1680/cien.2011.164.6.51`.

Arup, O. N. (1985). 1970 Key speech. *The Arup Journal* **20**.1, 34–36.

Ashwear, N. (2016). "Vibration-based assessment of tensegrity structures". PhD thesis. Stockholm, Sweden: Royal Institute of Technology.

Ashwear, N. and A. Eriksson (July 2014). Natural frequencies describe the pre-stress in tensegrity structures. *Computers & Structures* **138**, 162–171. DOI: `10.1016/j.compstruc.2014.01.020`.

Bach, K. (1977). *IL9: Pneus in Natur und Technik*. Vol. 9. Institut for Leichte Flächentragwerke (IL). Stuttgart: Institut for Leichte Flächentragwerke (IL). ISBN: 978-0815006633.

Balmond, C. (2007). *Informal*. Prestel.

Ban, S. (2000). Japanese pavilion at the EXPO in Hanover. *Detail* **40**.6, 1012–1017. ISSN: 0011-9571.

Barkhofen, E.-M. and A. Bögle (May 11, 2010). *High Energy. Ingenieur - Bau - Kultur - Structural Art - Jörg Schlaich Rudolf Bergermann*. Akademie der Künste.

Barnes, M. R. (1977). "Form finding and analysis of tension space structures by dynamic relaxation". PhD thesis. City University London.

Beauzamy, L., N. Nakayama, and A. Boudaoud (Oct. 2014). Flowers under pressure: ins and outs of turgor regulation in development. *Annals of Botany* **114**.7, 1517–1533.

Beghini, L. L. et al. (Nov. 2014). Structural optimization using graphic statics. *Structural and Multidisciplinary Optimization* **49**.3, 351–366. DOI: 10.1007/s00158-013-1002-x.

Bergdoll, B. (2000). *European Architecture 1750-1890*. Oxford University Press.

Block, P. and L. Lachauer (Mar. 2014). Three-dimensional funicular analysis of masonry vaults. *Mechanics Research Communications* **56**, 53–60. DOI: 10.1016/j.mechrescom.2013.11.010.

Block, P. (May 2009). "Thrust Network Analysis: exploring three-dimensional equilibrium". PhD dissertation. PhD thesis. Cambridge, MA, USA: Massachusetts Institute of Technology.

Block, P. and J. Ochsendorf (2007). Thrust network analysis: a new methodology for three-dimensional equilibrium. *Journal Of The International Association For Shell And Spatial Structures* **48**.3, 167–173.

Boyd, J. D. (1950). Tree growth stresses. II. The development of shakes and other visual failures in timber. *Australian Journal of Applied Science* **1**.3, 269–312.

Brandt, J. (1993). *The bicycle wheel*. 3rd. Avocet. ISBN: 9780960723669.

Brunner, J. (1921). Der Schweizerische Holzbrückenbau von 1750 bis 1850. *Schweizerische Bauzeitung* **78**.12, 139–141.

— (1924). "Beitrag zur geschichtlichen Entwicklung des Brückenbaues in der Schweiz". PhD thesis. ETH Zurich.

Bubner, E. (1975). *IL12: Convertible Pneus*. Vol. 12. Institut for Leichte Flächentragwerke (IL). Stuttgart: Institut for Leichte Flächentragwerke (IL). ISBN: 9780815007746.

Buchanan, A., B. Deam, et al. (May 2008). Multi-storey prestressed timber buildings in New Zealand. *Structural Engineering International* **18**.2, 166–173.

Buchanan, A., A. Palermo, et al. (Sept. 2011). Post-tensioned timber frame buildings. *The Structural Engineer* **89**.17, 24–30.

Burkhardt, B. (Mar. 2016). Natural structures - the research of Frei Otto in natural sciences. *International Journal of Space Structures* **31**.1, 9–15. DOI: 10.1177/0266351116642060.

Burkhardt, B. et al., eds. (1978). *IL13: Multihalle Mannheim*. Vol. 13. Institut for Leichte Flächentragwerke (IL). Stuttgart: Institut for Leichte Flächentragwerke (IL).

Calladine, C. R. (1978). Buckminster Fuller's "Tensegrity" structures and Clerk Maxwell's rules for the construction of stiff frames. *International Journal of Solids and Structures* **14**.2, 161–172. DOI: 10.1016/0020-7683(78)90052-5.

Candela, F. (1960). General formulas for membrane stresses in hyperbolic paraboloidical shells. *ACI Journal Proceedings* **57**.10, 353–371. DOI: `10.14359/8024`.

Cassens, D. L. and J. R. Serrano (Mar. 2004). "Growth Stress in Hardwood Timber". *Proceedings of the 14th Central Hardwood Forest Conference.* Ed. by D. A. Yaussy et al. Wooster, OH. Gen. Tech. Rep. NE-316. Newtown Square, PA: U.S. Department of Agriculture, Forest Service, Northeastern Research Station, pp. 106–115.

Casson, L. (1971). *Ships and seamanship in the Ancient World.* Princeton, New Jersey: Princeton University Press. ISBN: 0-691-03536-9.

Cauchy, A.-L. (1813). Sur les polygones et les polyèdres (second mémoire). *Journal de l'École polytechnique, XVIe cahier* **IX**, 87–89.

Charleson, A. W. and S. Pirie (2009). An investigation of structural engineer-architect collaboration. *Journal of the Structural Engineering Society of New Zealand* **22**.1, 97–104.

Chilton, J. (Sept. 25, 2020). "Physical models: Their historical and current use in civil and building engineering design". Ed. by B. Addis. Ernst, Wilhelm & Sohn. Chap. Heinz Isler and his use of physicalmodels, pp. 613–637. ISBN: 978-3-433-60962-0.

Christianson, J. and C. H. Marston (2015). *Covered bridges and the birth of American engineering.* Historic American Engineering Record National Park Service. ISBN: 978-0-578-17106-7.

Cohn-Vossen, S. (1927). Zwei Sätze über die Starrheit der Eiflächen. *Nachrichten von der Gesellschaft der Wissenschaften zu Göttingen. Mathematisch-Physikalische Klasse*, 125–134.

Corres-Peiretti, H. (June 2013). Sound engineering through conceptual design according to the fib Model Code 2010. *Structural Concrete* **14**.2, 89–98.

Corres, H. and J. Leon (Nov. 2012). Eminent structural engineer: Eduardo Torroja (1899–1961). *Structural Engineering International* **22**.4, 581–584. DOI: `10.2749/101686612X13363929517938`.

Cremona, L. (1872). *Le figure reciproche nella statica grafica.* ita. Tipografia di Giuseppe Bernardoni. DOI: `10.3931/e-rara-18757`.

Culmann, C. (1851). Der Bau der hölzernen Brücken in den Vereinigten Staaten von Nordamerika. *Allgemeine Bauzeitung* **16**, 69–129.

— (1866). *Die graphische Statik.* ger. Zürich: Meyer & Zeller. DOI: `10.3931/e-rara-20052`.

Curtain, B. et al. (2012). "Design of Carterton Event Centre: An example of innovative collaboration between architecture and timber engineering". *Proceedings of the 12th World Conference on Timber Engineering WCTE, Auckland, New Zealand.*

D'Aveni, A. and G. D'Agata (Oct. 2017). Post-tensioned timber structures: New perspectives. *Construction and Building Materials* **153**, 216–224.

Day, A. S. (1965). An introduction to dynamic relaxation. *The Engineer* **219**, 218–221. ISSN: 0013-7758.

Dechau, W. (2013). *Trutg dil Flem : sieben brücken von Jürg Conzett = Trutg dil Flem : seven bridges by Jürg Conzett.* Zurich: Scheidegger & Spiess. ISBN: 9783858813749.

Detail (2005). Berlin Hauptbahnhof – Lehrter Bahnhof. *Detail Magazine* 12, 1449–1455.

Diderot, D. and J. le Rond d'Alembert, eds. (1769). *Encyclopédie.* André le Breton et al.

Dixon, M. (Aug. 2015a). Frei Otto – inspired inventor, researcher and designer (part 1). *The Structural Engineer* 8, 12–17.

— (Sept. 2015b). Frei Otto – inspired inventor, researcher and designer (part 2). *The Structural Engineer* 9, 12–17.

Domokos, G. (1990). The equilibrium equations of membrane shells expressed in general surface coordinates. *Periodica Polytechnica Architecture* **34**.1–2, 85–134. URL: `https://pp.bme.hu/ar/article/view/2259`.

Drüsedau, H. (1983). *IL15: Lufthallenhandbuch.* Vol. 15. Institut for Leichte Flächentragwerke (IL). Stuttgart: Institut for Leichte Flächentragwerke (IL). ISBN: 9783782820158.

Edwards, S. A., J. Wagner, and F. Gräter (May 2012). Dynamic Prestress in a Globular Protein. *PLoS Computational Biology* **8**.5. Ed. by R. Nussinov.

Eisenhart, L. P. (1947). *An introduction to differential geometry, with use of the tensor calculus.* Princeton University Press.

Ekholm, K. (2013). "Performance of stress-laminated-timber bridge decks". PhD thesis. Chalmers University of Technology.

Engström, B. (2011). *Design and analysis of prestressed concrete structures.* Göteborg: Chalmers University of Technology.

Engström, D. et al. (2004). *Arkitektur och bärverk.* Ed. by D. Engström. Stockholm: Formas.

Evguenia, V. A. (Dec. 2016). "Open passage ethno-archaeology of skin boats and indigeneous maritime mobility of North-American Arctic". PhD thesis. University of Southampton.

Fabricius, D. (Nov. 2016). Architecture before architecture: Frei Otto's 'Deep History'. *The Journal of Architecture* **21**.8, 1253–1273.

Falk, A. and P. von Buelow (2009). "Combined timber plate and branching column systems – variations and development of system interaction". *Proceedings of the International Association for Shell and Spatial Structures (IASS) Symposium 2009, Valencia*, pp. 999–1010.

Fivet, C. (2021). *Building out of concrete, but without pouring concrete.* URL: `https://actu.epfl.ch/news/building-out-of-concrete-but-without-pouring-concr/` (visited on 10/12/2021).

Frampton, K. (2007). *Modern Architecture: A Critical History.* Fourth Edition. World of Art. Thames & Hudson.

Frampton, K. and Y. Futagawa (1983). *Modern Architecture 1851-1945.* Rizzoli.

Fraternali, F. (Mar. 2010). A thrust network approach to the equilibrium problem of unreinforced masonry vaults via polyhedral stress functions. *Mechanics Research Communications* **37**.2, 198–204. DOI: `10.1016/j.mechrescom.2009.12.010`.

Fuller, R. B. (1962). "Tensile-integrity structures". U.S. pat. 3063521.

Galiano, L. (2020). *AV Monographs 222: Heatherwick Studio 2000-2020.* Madrid: Arquitectura Viva SL. ISBN: 9788409196340.

Gans, D., ed. (1991). *Bridging the gap: rethinking the relationship between architect and engineer.* Van Nostrand Reinhold. ISBN: 0-442-00135-5.

Gasparini, D. A., J. Bruckner, and F. da Porto (2006). Time-dependent behavior of posttensioned wood Howe bridges. *Journal of Structural Engineering* **132**.3, 418–429.

Gasparini, D. A. and F. da Porto (Jan. 2003). "Prestressing of the 19th century wood and iron truss bridges in the U.S." *Proceedings of the First International Congress on Construction History*. Ed. by S. Huerta. Vol. III. Madrid: Instituto Juan de Herrera, SEHC, COAC, CAATC, pp. 977–986.

Gasparini, D. A. and C. Provost (1989). Early nineteenth century developments in truss design in Britain, France and the United States. *Construction History* **5**.

Gasparini, D. A. and D. Simmons (1997). American Truss Bridge Connections in the 19th Century. I: 1829—1850. *Journal of Performance of Constructed Facilities* **11**.3, 119–129.

Glaeser, L. (1972). *The work of Frei Otto*. Museum of Modern Art; distributed by New York Graphic Society, Greenwich, Conn. ISBN: 0870703323.

Gordon, J. E. (1978). *Structures : or Why things don't fall down*. Harmondsworth: Penguin. ISBN: 0-14-021961-7.

Graefe, R. (Sept. 25, 2020). "Physical models: Their historical and current use in civil and building engineering design". Ed. by B. Addis. Ernst, Wilhelm & Sohn. Chap. The catenary and the line of thrust as a means for shaping arches and vaults, pp. 79–126. ISBN: 978-3-433-60962-0.

Graefe, R. and J. Tomlow (1990). *Vladimir G. Suchov 1853-1939; Die Kunst Der Sparsamen Konstruktion*. Stuttgart: Deutsche Verlags-Anstalt. ISBN: 3-421-02984-9.

Granello, G. et al. (Aug. 2018). Design approach to predict post-tensioning losses in post-tensioned timber frames. *Journal of Structural Engineering* **144**.8.

Green, A. E. and W. Zerna (1968). *Theoretical elasticity*. 2nd ed. Oxford University Press. ISBN: 0486670767.

Greenwold, S. and E. Allen (2003). *Active statics*. URL: `http://acg.media.mit.edu/people/simong/statics/data/`.

Haegermann, G., G. Huberti, and H. Möll (1964). *Vom Caementum zum Spannbeton*. Ed. by G. Huberti. Vol. 1. part A-C. Berlin: Bauverlag.

Hanaor, A. (1994). Geometrically rigid double-layer tensegrity grids. *International Journal of Space Structures* **9**.4, 227–238.

Happold, E. and W. I. Liddell (Mar. 1975). Timber lattice roof for the Mannheim Bundesgartenschau. *The Structural Engineer* **53**.3, 99–135.

Hellström, B., H. Granholm, and G. Wästerlund, eds. (1958). *Betong - del 1*. 2nd ed. Natur och Kultur.

Heyman, J. (1966). The stone skeleton. *International Journal of Solids and Structures* **2**.2, 249–279. DOI: `10.1017/cbo9781107050310`.

Hitz, Z. (May 26, 2020). *Lost in thought: the hidden pleasures of an intellectual life*. Princeton university press. 240 pp. ISBN: 9780691178714. URL: `https://www.ebook.de/de/product/38169249/zena_hitz_lost_in_thought_the_hidden_pleasures_of_an_intellectual_life.html`.

Hooke, R. (1675). *A description of helioscopes, and some other instruments*. London.

Howe, W. (Aug. 1840). "Manner of constructing the truss-frames of bridges and other structures." U.S. pat. 1711.

Hsu, C.-S. (Oct. 1960). Generalization of Cohn-Vossen's theorem. *Proceedings of the American Mathematical Society* **11**.5, 845. DOI: `10.2307/2034571`.

Huerta, S. (Dec. 2006). Structural design in the work of Gaudí. *Architectural Science Review* **49**.4, 324–339. ISSN: 0003-8628. DOI: `10.3763/asre.2006.4943`.

Jackson, P. H. (Apr. 1886). "Forming artificial-stone or concrete arches". English. U.S. pat. US339296.

Jacobs, M. R. (1938). The fiber tension of woody stems with special reference to the genus Eucalyptus. *Commonwealth Forestry Bureau* 22.

James, J. G. (1982). The evolution of wooden bridge trusses to 1850. *Journal of the Institute of Wood Science*, 116–135, 168–193. ISSN: 0020-3203.

Johnson, J. B., F. E. Turneaure, and C. W. Bryan (1894). *The theory and practice of modern framed structures – Designed for the use of schools and for engineers in professional practice*. Third edition. New York: John Wiley & Sons.

Johnson, S. (Feb. 2015). *BIG and Heatherwick Studio design a new Google headquarters*. URL: `https://www.architectmagazine.com/design/big-and-heatherwick-studio-design-a-new-google-headquarters_o` (visited on 06/14/2021).

Kärrholm, G. and A. Samuelsson (1972). Analysis of a prestressed cable-roof anchored in a space-curved ring beam. *IABSE congress report* 9.

Kaylor, H. (1961). *Prestressed concrete simply explained*. London: Contractors Record.

Kil'chevskiĭ, N. A. (1965). *Fundamentals of the analytical mechanics of shells*. NASA TT F-292. Washington, D.C.: NASA TT F-292.

Killer, J. (1942). "Die Werke der Baumeister Grubenmann: eine baugeschichtliche und bautechnische Forschungsarbeit". PhD thesis. ETH Zürich.

Knoll, F. (1989). "La pyramide du Grand Louvre". *IABSE Periodica P131/89*. Vol. 1. IABSE.

Krauth, T. and F. S. Meyer (1893). *Die Bau- und Kunstzimmerei - Erster Band : Text*. Kanter & Mohr.

Krieg, M., A. R. Dunn, and M. B. Goodman (Feb. 2014). Mechanical control of the sense of touch by β-spectrin. *Nature Cell Biology* **16**.3, 224–233.

Krishna, P. and P. Godbole (2013). *Cable-suspended roofs*. Second edition. Tata Mcgraw Hill Education Private Limited. ISBN: 9781259028472.

Krizmanić, A. (Dec. 2020). Amfiteatar u Puli; Velarium. *Prostor* **28**.2 (60), 202–219. DOI: `10.31522/p.28.2(60).1`.

Kubler, H. (1987). Growth stresses in trees and related wood properties. *Forestry abstracts* **48**, 131–189.

Kullmann, E., W. Nachtigall, and J. Schurig (1975). *IL8: Netze in Natur und Technik*. Ed. by K. Bach. Vol. 8. Institut for Leichte Flächentragwerke (IL). Stuttgart: Institut for Leichte Flächentragwerke (IL). ISBN: 9783782820080.

Kurrer, K.-E. (2008). *The history of the theory of structures: from arch analysis to computational mechanics*. first. Ernst & Sohn. ISBN: 978-3-433-01838-5.

Origins of tensegrity: views of Emmerich, Fuller and Snelson (1996). *International Journal of Space Structures* **11**.1–2. Ed. by H. Lalvani, 27–55.

Larsen, O. P. and A. Tyas (2003). *Conceptual structural design: bridging the gap between architects and engineers*. Thomas Telford Publishing. ISBN: 0727732358.

Lenczner, E. A. R. (June 1994). The design of the stone facade to the Pavilion of the Future, Expo '92, Seville. *The Structural Engineer* **72**.11, 171–177.

Leonhardt, F. (1964). *Prestressed Concrete; Design and Construction*. Second. Berlin: Wilhelm Ernst and Sohn.

Liddell, W. I. and P. Westbury (Aug. 1999). Design and construction of the Millennium Dome, UK. *Structural Engineering International* **9**.3, 172–175. DOI: 10.2749/101686699780482023.

Linkwitz, K. and H.-J. Schek (1971). Einige Bemerkungen zur Berechnung von vorgespannten Seilnetzkonstruktionen. *Ingenieur-Archiv* **40**.3, 145–158.

Liu, Y., B. Zwingmann, and M. Schlaich (Oct. 2015). Carbon fiber reinforced polymer for cable structures—a review. *Polymers* **7**.10, 2078–2099. DOI: 10.3390/polym7101501.

Long, S. H. (Mar. 1830). "Wooden-framed brace-bridges". English. U.S. pat. 5862X.

— (Nov. 1839). "Improvement in wooden-framed brace-bridges". English. U.S. pat. US1398.

Lozano-Galant, J. A. and I. Paya-Zaforteza (Nov. 2017). Analysis of Eduardo Torroja's Tempul Aqueduct an important precursor of modern cable-stayed bridges, extradosed bridges and prestressed concrete. *Engineering Structures* **150**, 955–968. DOI: 10.1016/j.engstruct.2017.07.057.

Luchsinger, R. H., M. Pedretti, and A. Reinhard (Dec. 2004). Pressure induced stability: from pneumatic structures to Tensairity. *Journal of Bionic Engineering* **1**.4, 141–148. DOI: 10.1007/bf03399470.

Lund, J. G. F. (June 1912). "Means for positioning building parts or elements". English. U.S. pat. US1028578.

Mattheck, C. and H. Kubler (1995). *Wood - The Internal Optimization of Trees*. Springer Series in Wood Science. Springer. ISBN: 3540593187.

Mattheck, C. and I. Tesari (2004). "The mechanical self-optimisation of trees". *Design and Nature II*. Ed. by M. Collins and C. A. Brebbia. Vol. 73. WIT Transactions on Ecology and the Environment. WIT Press, pp. 197–206.

Maxwell, J. C. (Apr. 1864a). On reciprocal figures and diagrams of forces. *The London, Edinburgh, and Dublin Philosophical Magazine and Journal of Science* **27**.182, 250–261. DOI: 10.1080/14786446408643663.

— (1864b). On the calculation of the equilibrium and stiffness of frames. *Philosophical Magazine Series 4* **27**.182, 294–299. DOI: 10.1080/14786446408643668.

— (1870). On reciprocal figures, frames, and diagrams of forces. *Transactions of the Royal Society of Edinburgh* **26**.1, 1–40. DOI: 10.1017/s0080456800026351.

McConnell, E., D. McPolin, and S. Taylor (Dec. 2014). Post-tensioning of glulam timber with steel tendons. *Construction and Building Materials* **73**, 426–433.

McRobie, A. (June 2016). Maxwell and Rankine reciprocal diagrams via Minkowski sums for two-dimensional and three-dimensional trusses under load. *International Journal of Space Structures* **31**.2-4, 203–216. DOI: 10.1177/0266351116660800.

Menn, C. (1990). *Prestressed concrete bridges*. Ed. by P. Gauvreau. Basel: Birkhäuser. ISBN: 978-3-0348-9920-8. DOI: 10.1007/978-3-0348-9131-8.

Miki, M. et al. (Dec. 2020). Form-finding of shells containing both tension and compression using the Airy stress function. *Preprint*. DOI: 10.20944/preprints202012.0355.v2.

Miller, J. F. (2009). "Design and analysis of mechanically laminated timber beams using shear keys". PhD thesis. Michigan Technological University.

Möbius, A. F. (1837). *Lehrbuch der statik*. Vol. 2. Leipzig: G.J. Göschen.

Mortimer, B. et al. (Sept. 2016). Tuning the instrument: sonic properties in the spider's web. *Journal of The Royal Society Interface* **13**.122, 20160341. DOI: `10.1098/rsif.2016.0341`.

Motro, R. and V. Raducanu (2003). Tensegrity systems. *International Journal of Space Structures* **18**.2, 77–84.

Motro, R. (Dec. 2007). Robert Le Ricolais (1894–1977) " Father of Spatial Structures". *International Journal of Space Structures* **22**.4, 233–238. DOI: `10.1260/026635107783133834`.

Münch, E. (1938). Statik und Dynamik des schraubigen Baues der Zellwand, besonders des Druck- und Zugholzes. *Flora oder Allgemeine Botanische Zeitung* **132**.4, 357–424. ISSN: 0367-1615. DOI: `10.1016/S0367-1615(17)31909-2`. URL: `http://www.sciencedirect.com/science/article/pii/S0367161517319092`.

NCK (n.d.). *NCK: Pyramide du Grand Louvre*. Accessed: 2016-12-02. URL: `http://www.nck.ca/fr/projects/pyramide_louvre.php`.

Nervi, P. L. (1956). *Structures*. McGraw-Hill Book Company.

Newcombe, M. P. (2011). "Seismic design of post-tensioned timber frame and wall buildings". PhD thesis. University of Canterbury.

Nielsen, J. (1964). Kræfter i gitterflader – Forces in space frames. *Nordisk Betong* **8**.4, 465–484.

Nsugbe, E. and C. J. K. Williams (1999). Robert Le Ricolais—Visions and Paradox: AA Exhibition Gallery 11 January – 5 February 1999. *AA Files* 39, 55–60. ISSN: 0261-6823. URL: `http://www.jstor.org/stable/29544157`.

Nutbourne, A. W. (1986). "A circle diagram for local differential geometry". *The Mathematics of surfaces: The proceedings of a conference organized by the Institute of Mathematics and its Applications and held at the University of Manchester, 17-19 September 1984*. Ed. by J. A. Gregory. Oxford: Oxford University Press, pp. 59–71. ISBN: 0198536097.

Oakeshott, R. E. (1960). *The archeology of weapons: arms and armour from prehistory to the age of chivalry*. London: Lutterworth Press.

Ochsendorf, J. and J. Antuña (Jan. 2003). "Eduardo Torroja and «Cerámica Armada»". *Proceedings of the First International Congress on Construction History*. Ed. by S. Huerta. Vol. III. Madrid: Instituto Juan de Herrera, pp. 1527–1536.

Oliva, M. G. et al. (1990). Stress-laminated wood bridge decks: experimental and analytical evaluations. Res. pap. FPL-RP-495. *U.S. Department of Agriculture, Forest Service, Forest Products Laboratory*.

Olsson, K.-G. and O. Dahlblom (2016). *Structural mechanics: Modelling and analysis of frames and trusses*. John Wiley and Sons Ltd.

Otto, F. (1954). *Das hängende Dach: Gestalt und Struktur*. Bauwelt verlag.

— (1995). *IL35: Pneu and Bone*. Ed. by F. Klenk. Vol. 35. Institut for Leichte Flächentragwerke (IL). Stuttgart: Karl Krämer Verlag. ISBN: 3-7828-2035-5.

Otto, F. and B. Rasch (1995). *Frei Otto, Bodo Rasch : finding form : towards an architecture of the minimal*. [Stuttgart]: Axel Menges.

Palermo, A. et al. (2005). "Seismic design of multi-storey buildings using laminated veneer lumber (LVL)". *Proceedings of New Zealand Society for Earthquake Engineering Conference*. Wairakei, New Zealand.

Patterson, M. (Apr. 2011). *Structural glass facades and enclosures*. Wiley. ISBN: 978-0-470-50243-3.

Pedretti, M. and R. Luscher (May 2007). Tensairity-patent - Eine pneumatische tenso-struktur. *Stahlbau* **76**.5, 314–319. DOI: 10.1002/stab.200710037.

Pellegrino, S. (Jan. 1986). "Mechanics of kinematically indeterminate structures". PhD thesis. University of Cambridge.

Pellegrino, S. and C. R. Calladine (1986). Matrix analysis of statically and kinematically indeterminate frameworks. *International Journal of Solids and Structures* **22**.4, 409–428.

Perez-Sala, J. C. et al. (2018). "Exploration of externally post-tensioned spatial structures using 3D graphic statics". *Proceedings of the International Association for Shell and Spatial Structures (IASS) Symposium 2018*. Ed. by C. Mueller and S. Adriaenssens.

Pratt, T. W. and C. Pratt (Apr. 1844). "Truss-frame of bridges". U.S. pat. 3523.

Pucher, A. (1938). Die Berechnung der Dehnungsspannungen von Rotationsschalen mit Hilfe von Spannungsfunktionen. *International Association for Bridge and Structural Engineering Publications* **5**, 275–299. DOI: 10.5169/seals-6163.

Pugh, A. (1976). *An introduction to tensegrity*. The Dome series. University of California Press.

Rankine, W. J. M. (1858). *A manual of applied mechanics*. Encyclopaedia metropolitana. London and Glasgow: Richard Griffin and CO.

Rice, P. (1996). *An Engineer Imagines*. 2nd ed. London: Elipsis.

Rippmann, M., L. Lachauer, and P. Block (Dec. 2012). Interactive vault design. *International Journal of Space Structures* **27**.4, 219–230. DOI: 10.1260/0266-3511.27.4.219.

Rippmann, M., T. Van Mele, et al. (Sept. 2016). "The Armadillo Vault: computational design and digital fabrication of a freeform stone shell". *Advances in Architectural Geometry 2016*, pp. 344–363.

Rogers, C. and W. K. Schief (June 2002). *Bäcklund and Darboux Transformations*. Cambridge University Press. DOI: 10.1017/cbo9780511606359.

Safaei, S. D. (2012). "Stiffness and vibration properties of slender tensegrity strucutres". PhD thesis. Stockholm: Royal Institute of Technology. ISBN: 978-91-7501-461-6.

Samuelsson, S. (2015). *Ingenjörens konst*. Balkong förlag.

Sanabra-Loewe, M. and J. Capellà-Llovera (Sept. 2014). The four ages of early prestressed concrete structures. *PCI Journal* **59**.4, 93–121.

Schek, H.-J. (1974). The force density method for form finding and computation of general networks. *Computer Methods in Applied Mechanics and Engineering* **3**.1, 115–134. ISSN: 0045-7825. DOI: 10.1016/0045-7825(74)90045-0.

Schlaich, J. and M. Schlaich (Sept. 2008). *Lightweight structures*. URL: https://architecture.mit.edu/sites/architecture.mit.edu/files/attachments/lecture/LightweightStructures.pdf (visited on 09/11/2020).

Schlaich, J., H. Schober, and T. Helbig (2001). Eine verglaste Netzschale: Dach und Skulptur - DG bank am Pariser Platz in Berlin. *Bautechnik* **78**.7, 457–463.

Schlaich, M. (2004). The Messeturm in Rostock – a tensegrity tower. *Journal of the International Association for Shell and Spatial Structures* **45**.2. n. 145, 93–98.

Schlaich, M. (Mar. 2018). Frei Otto – reverberation at schlaich bergermann partner. *Journal of the International Association for Shell and Spatial Structures* **59**.1. n. 195, 43–54. DOI: 10.20898/j.iass.2018.195.902.

Schlaich, M. and R.-M. Behnke (June 2014). Selbstverankerte Seilnetze – ein leichtes Dach in der Autostadt in Wolfsburg. *Bauingenieur* **89**.6, 235–245. ISSN: 0005-6650.

Schober, H. and J. Schneider (May 2004). Developments in structural glass and glass structures. *Structural Engineering International* **14**.2, 84–87. DOI: 10.2749/101686604777964044.

Sehlström, A. (Aug. 2019). "Prestress in nature and technics". Thesis for the degree of Licentiate of Engineering in Architecture. PhD thesis. Chalmers University of Technology. URL: https://research.chalmers.se/publication/511695.

Sehlström, A., M. Ander, and K.-G. Olsson (2021). "Architectural design methods used in engineering Master's thesis projects". *KUL2021: Chalmers Konferens om Undervisning och Lärande.*

Skelton, R. E. et al. (2001). "An introduction to the mechanics of tensegrity structures". *Proceedings of the 40th IEEE Conference on Decision and Control (Cat. No.01CH37228).* IEEE.

Snelson, K. (June 2012). The art of tensegrity. *International Journal of Space Structures* **27**.2-3, 71–80.

— (2013). *Art and ideas.* Web Publication: Kenneth Snelson. URL: http://www.lulu.com/shop/kenneth-snelson/kenneth-snelson-art-and-ideas/ebook/product-21038507.html.

Southwell, R. V. (Feb. 1920). Primary stress-determination in space frames. *Engineering* 109, 165–168.

Struik, D. J. (1961). *Lectures on classical differential geometry.* Second edition. Dover.

Sutherland, R. J. M. (1997). *Structural iron 1750–1850.* Routledge. ISBN: 9780860787587.

— (2001). *Historic concrete: background to appraisal.* London Reston, VA: Thomas Telford. ISBN: 9780727728753.

Thompson, D. W. (1942). *On growth and form.* Second. Cambridge University Press. ISBN: 9781371927387.

Tibert, G. (Apr. 2002). "Deployable tensegrity structures for space applications". PhD thesis. Stockholm: Royal Institute of Technology.

Tibert, G. and S. Pellegrino (Apr. 2003). "Deployable tensegrity masts". *44th AIAA/ASME/ASCE/AHS/ASC Structures, Structural Dynamics, and Materials Conference.* American Institute of Aeronautics and Astronautics. DOI: 10.2514/6.2003-1978.

Timoshenko, S. and S. Woinowsky-Krieger (1959). *Theory of Plates and Shells.* Second edition. McGraw-Hill book company. ISBN: 0-07-064779-8.

Todisco, L. (Mar. 2016). "Funicularity and equilibrium for high-performance conceptual structural design". PhD thesis. Technical University of Madrid, School of Civil Engineering. URL: http://oa.upm.es/39733/.

Todisco, L. et al. (Dec. 2015). Design and exploration of externally post-tensioned structures using graphic statics. *Journal of the International Association for Shell and Spatial Structures* **56**.4, 249–258. ISSN: 1028-365X.

Tomlow, J. (Mar. 2016). Designing and constructing the Olympic roof (Munich 1972). *International Journal of Space Structures* **31**.1, 62–73.

Torr, C. (1895). *Ancient ships*. Cambridge: University Press. URL: https://archive.org/details/ancientships00torruoft.

Torroja, E. (Oct. 1948). The Alloz aqueduct, Spain: A prestressed watertight structure. *Concrete and Constructunal Engineering* **43**, 315–316. ISSN: 0366-550X.

— (Feb. 1962). Acueducto de Tempul. *Informes de la Construcción* **14**.137, 135–140. DOI: 10.3989/ic.1962.v14.i137.4943.

Trout, E. (Sept. 25, 2020). "Physical models: Their historical and current use in civil and building engineering design". Ed. by B. Addis. Ernst, Wilhelm & Sohn. Chap. Scale models for structural testing at the Cement and Concrete Association, UK: 1951-1973, pp. 511–549. ISBN: 978-3-433-60962-0. DOI: 10.1002/9783433609613.ch17.

UN Environment and International Energy Agency (2017). Towards a zero-emission, efficient, and resilient buildings and construction sector: Global status report 2017.

Van Mele, T. and P. Block (2014). Algebraic graph statics. *Computer-Aided Design* **53**, 104–116. DOI: 10.1016/j.cad.2014.04.004.

Van Mele, T., C. Brunier-Ernst, and P. Block (2009). *eQUILIBRIUM - interactive, graphic statics-based structural design*. URL: https://block.arch.ethz.ch/equilibrium/ (visited on 02/06/2019).

Varignon, P. (1725). *Nouvelle mécanique ou statique: dont le projet fut donné en M.DC. LXXXVII / ouvrage posthume de … Varignon*. 1st ed. Paris: Claude Jombert.

Veenendaal, D. and P. Block (Dec. 2012). An overview and comparison of structural form finding methods for general networks. *International Journal of Solids and Structures* **49**.26, 3741–3753. DOI: 10.1016/j.ijsolstr.2012.08.008.

Viollet-le-Duc, E.-E. (1881). *Lectures on architecture*. Vol. 2. Lectures on Architecture. Sampson Low, Marston, Searle and Rivington.

Vitruvius, M., M. H. Morgan, and H. L. Warren (1914). *Vitruvius: The Ten Books on Architecture*. Cambridge: Harvard University Press.

Vrachliotis, G. (2017). *Frei Otto, Carlfried Mutschler: Multihalle*. Spector Books. ISBN: 978-3-95905-192-7.

Wanninger, F. and A. Frangi (July 2014). Experimental and analytical analysis of a post-tensioned timber connection under gravity loads. *Engineering Structures* **70**, 117–129.

— (Apr. 2016). Experimental and analytical analysis of a post-tensioned timber frame under horizontal loads. *Engineering Structures* **113**, 16–25.

Wanninger, F. (2015). "Post-tensioned timber frame structures". PhD thesis. ETH Zürich.

Weinand, Y. (2016). *Projekt Grubenmann / Grubenmann Project*. Ed. by S. Grubenmann-Sammlung. Verlagsgenossenschaft St. Gallen. ISBN: 978-3-7291-1153-0.

Wells, M. (2010). *Engineers: a history of engineering and structural design*. Routledge. ISBN: 0-415-32526-9.

Wilkins, A. P. (Jan. 1986). Nature and origin of growth stresses in trees. *Australian Forestry* **49**.1, 56–62.

Williams, C. J. K. (2001). "The analytic and numerical definition of the geometry of the British Museum Great Court Roof". English. *The proceedings of mathematics and design 2001*. Ed. by M. Burry et al. Deakin University, Geelong, Victoria 3217, Australia, pp. 334–440. ISBN: 0730025268.

Williams, C. J. K. (June 2011). Patterns on a surface: the reconciliation of the circle and the square. *Nexus Network Journal* **13**.2, 281–295. DOI: 10.1007/s00004-011-0068-2.

Williams, C. J. K. and A. McRobie (June 2016). Graphic statics using discontinuous Airy stress functions. *International Journal of Space Structures* **31**.2-4, 121–134. DOI: 10.1177/0266351116660794.

Wise, C. et al. (June 2012). An amphitheatre for cycling: the design, analysis and construction of the London 2012 Velodrome. *The Structural Engineer*, 13–25.

Wroldsen, A. S. (2007). "Modelling and control of tensegrity structures". PhD thesis. Norwegian University of Science and Technology.

Wu, M. and M. Sasaki (Apr. 2007). Structural behaviors of an arch stiffened by cables. *Engineering Structures* **29**.4, 529–541. DOI: 10.1016/j.engstruct.2006.05.018.

Yang, J. (2019). "Flexural strengthening of reinforced concrete beams using externally bonded CFRP: An innovative method for the application of prestressed CFRP laminates". licthesis. Göteborg: Chalmers University of Technology.

Zieta, O., P. Dohmen, and U. Teutsch (2008). Verformtes Blech. *TEC21* **134**.17-18, 35–39. DOI: 10.5169/seals-108919.

Zwerger, K. (2000). *Wood and wood joints : building traditions of Europe and Japan*. Birkhauser. ISBN: 3-7643-6333-9.

List of Figures